

Delta-method applied to the temperature and precipitation time series - An example

Title	Delta-method applied to the temperature and precipitation time series - An example
Creator	C3i, University of Geneva
Creation date	February 2012
Date of last revision	March 2012
Subject	Create spatially explicit scenarios on climate change
Status	Finalized
Type	Technical document
Description	Overview of available datasets and description of a technique to produce climate scenarios relevant to impact studies in the Black Sea Catchment.
Contributor(s)	Ana Gago da Silva, Ian Gunderson, Stéphane Goyette and Anthony Lehmann
Rights	
Identifier	enviroGRIDS_D3.6
Language	English
Relation	enviroGRIDS_D3.7, enviroGRIDS_D3.8

Abstract

This document describes the results of the spatially explicit scenarios on climate change for the Black Sea catchment (Task 3.6) of WP3. A methodology devised to compute the temperature and precipitation changes according to Regional Climate Model (RCM) simulated outputs is described and applied to existing meteorological station observations, and to Climatic Research Unit (CRU) weather station derived gridded precipitation and temperature datasets. The model outputs selected for the development of this methodology are those of the Danish RCM called HIRHAM. This methodology aims at perturbing observed time series with changes allowing increasing as a function of time. These changes are based on the partial differences of the monthly probability distribution function (PDF). The partitions are chosen to be some quantiles of the PDF and these have been found to give better results if they divide the distribution into ten equal parts, or “deciles”; this approach of gradually perturbing observations with such specific differences is termed in the scientific literature as “delta-method”. This version of the delta-method (DM) was applied to a subset of meteorological stations in the Black Sea catchment and also to the CRU gridded temperature and precipitation datasets. The results obtained after applying the DM to both meteorological stations and the CRU point variables, show that the predicted minimum and maximum temperatures distributions are close to those found in the meteorological records and of the CRU point values for the current climate period. Then, beyond the observation periods at the end of the 21st century, the DM reproduces realistically the temperature and precipitation evolution corresponding to the HIRHAM climate simulations. However the comparison between the observed period of both CRU and closest HIRHAM grid point, suggests that the CRU data does not reproduce accurately both temperature and precipitation. In conclusion the results obtained show that the DM should give satisfying results for an extended time series, when considering the monthly variability. Finally, some general recommendations as regards to the meteorological inputs for SWAT users are provided at the end of this document.

Table of Contents

ABSTRACT.....	2
1 INTRODUCTION.....	5
2 DATA.....	6
2.1 REGIONAL CLIMATE MODEL OUTPUTS.....	6
2.2 METEOROLOGICAL STATIONS OBSERVATION DATASETS	7
2.3 CRU DATASET	8
3 METHODOLOGY	9
3.1 TEMPERATURE	11
3.2 PRECIPITATION.....	13
4 RESULTS	15
4.1 METEOROLOGICAL STATIONS.....	15
4.1.1 Temperature.....	15
4.1.2 Precipitation.....	19
4.2 CRU DATASET	29
4.2.1 Temperature.....	30
4.2.2 Precipitation.....	34
5 DISCUSSION AND CONCLUSION.....	37
6 RECOMMENDATIONS FOR SWAT.....	38
7 REFERENCES.....	40

List of figures

Figure 1 : HIRHAM surface grid mesh – Black Sea catchment	6
Figure 2 : Subset of Meteorological Stations providing observed datasets – Black Sea catchment.....	7
Figure 3 : CRU Grid Points – Black Sea catchment	8
Figure 4 : Closest HIRHAM grid points to a subset of meteorological stations observations datasets.....	10
Figure 5: Closest PRUDENCE grid points to the CRU grid points selected for the Black Sea catchment.....	10
Figure 6: T_{max} and T_{min} measured at meteorological station in Austria	15
Figure 7 : Averaged daily temperature distributions for weather station ID 112700 and associated HIRHAM RCM grid point Grid point ID (long=30, lat=44) located in Austria.	16
Figure 8: Frequency distributions of observed T_{min} and T_{max} for meteorological station ID 112700 (1976-2005).17	
Figure 9: Frequency distributions of simulated T_{min} and T_{max} for HIRHAM grid point (long=30, rlat=44), during the control period (HC1 – 1961-1990) and both SRES scenarios, HB1 (B2) and HS1 (A2) – 2071-2100.....	17
Figure 10: Frequency distributions of predicted T_{min} and T_{max} at Meteorological Station "112700", according to both SRES scenarios HB1 (B2) and HS1 (A2) – 2071-2100.	18
Figure 11: Precipitation Meteorological Station ID 339460_p situated in Crimea	19
Figure 12: Precipitation values for HC1, HS1 and HB1 PRUDENCE Scenarios, Grid Point ID (lon=77, lat=24)	20
Figure 13: Precipitation values for HC1, HS1 and perturbed HC1 (preliminary perturbation of HC1), Grid Point ID (long,rlat)=(77,24)	21
Figure 14: Precipitation values for HC1, HS1 and perturbed HC1 (final perturbation of HC1), Grid Point ID (lon=77, lat=24)	22
Figure 15: Observations and climate scenarios percentiles: station ID 111650_p and 339460_p	24
Figure 16: Precipitation time series for station ID 111650_p	25
Figure 17: Percentage of Wet Days and Average Monthly Precipitation for Station ID 111650_p.....	26
Figure 18: Precipitation time series at meteorological station ID 339460_p	27
Figure 19: Percentage of Wet Days and Average Monthly Precipitation for Station ID 339460_p.....	28
Figure 20: CRU gridpoints - Selected gridpoints	29
Figure 21: T_{min} , T_{max} averages for CRU ID Point 2619_t.....	31
Figure 22: Temperature frequency distribution of Observation period and Predicted scenarios, CRU ID point 2619_t	32
Figure 22: Temperature frequency distribution of PRUDENCE RCM, CRU ID point 2619_t	33
Figure 23 : Precipitation percentiles values for January at CRU point ID 5459_p	34
Figure 24 : Precipitation time series for CRU point ID 5459_p.....	35
Figure 25: Percentage of wet days and monthly average precipitation at CRU point ID 5459_p.....	36

List of Tables

Table 1: Averages and standard deviations of control, future scenarios and final results, gridpoint id (lon=77, lat=,24). HC1=Control, HS1=A2 and HB1=B2	19
--	----

1 Introduction

The methodology used in this work follows the steps described in the Deliverable 3.2, “Existing data access and compilation on regional climate, historical records and prospects model of the enviroGRIDS project” (Goyette, 2010). The objective of this work aims to perturb the observed series of daily maximum and minimum temperature, and daily precipitation in the Black Sea catchment according to the Delta-Method (DM). The perturbation entering in this method are computed on the basis of Regional Climate Models (RCMs) temperature and precipitation outputs from the PRUDENCE project using IPCC SRES A2 and B2 Green House Gas (GHG) emission scenarios (Nakicenovic et al., 2000). In addition, another set of observations obtained from the grid points of the Climatic Research Unit (CRU) dataset were also used¹.

The DM has been used in different studies as it is known to give reasonable results for the mean characteristics of future temperature and precipitation (Fowler et al., 2007; Lenderink et al., 2007). The assumption underlying the DM is that RCMs simulate relative changes more reliably than absolute values (Hay *et al.*, 2000). In previous studies, Global Climate Model (GCMs) outputs were used as the data to be downscaled (Hay *et al.*, 2000; Diaz-Nieto and Wilby, 2005; Quilbe *et al.*, 2008). In this study, climatic data was simulated with RCMs, not from GCMs as it was the case in the past.

The DM is also known for bias removal, since it is based on differences and ratios between current and future simulated climates, assuming that biases are systematic (Lenderink *et al.*, 2007; Bosshard *et al.*, 2011). This study follows the recommendations of previous studies (Murphy, 1999; Murphy, 2000; Diaz-Nieto and Wilby, 2005) through the convergence of the two downscaling techniques by using the DM alongside Statistical Downscaling techniques (SDS) using their advantages in a complementary way. This will hopefully contribute to the acquisition of more realistic and applicable future scenarios useful for the Soil Water Assessment Tool hydrological model (SWAT) and therefore contribute to buildings predictions of future water resources.

¹ CRU <http://www.cru.uea.ac.uk>

2 Data

2.1 Regional Climate Model outputs

The RCM outputs used during this work were simulated with the Danish RCM HIRHAM, driven by the United Kingdom's Hadley Center HadAM3H GCM outputs. This model had been used under the scope of the Fifth Research Framework Program of the European Union, the PRUDENCE project (Christensen and Christensen, 2007b). The majority of the data produced by this project are freely available².

HIRHAM was first run to simulate data for a control period (HC), from 1961 to 1990. A number of potential future climates were also simulated for the period of 2071 to 2100 (HS and HB), representing two IPCC's SRES GHG emission scenarios (Nakicenovic *et al.*, 2000). The HS scenario corresponds to the IPCC's SRES A2 scenario, while the HB scenario represents the SRES B2 scenario. These two periods were run a number of times using slightly different model configuration each time for PRUDENCE, but only the data from the first run was used, HC1, HS1 and HB1. Different model diagnostics were available, varying from seasonal, to monthly, to daily. Daily values were used in order to use the DM in an optimal manner. Eighteen different variables representing climatic data were also available. This study focuses on precipitation, and minimum and maximum air temperature at 2 meters above the surface (respectively RCM Pcp, RCM T_{min} and RCM T_{max}); these were downloaded from the PRUDENCE website in netCDF format. These variables were chosen to best represent the needs of the enviroGRIDS project focusing on sustainable development and to be potentially useful for SWAT, also used in the project. In the case of the HIRHAM model, the netCDF for each variable and period contain 10 800 daily values, corresponding to 360 days for a 30 year period, for each of the 7560 grid points present at the surface of the computational grid (Fig. 1).

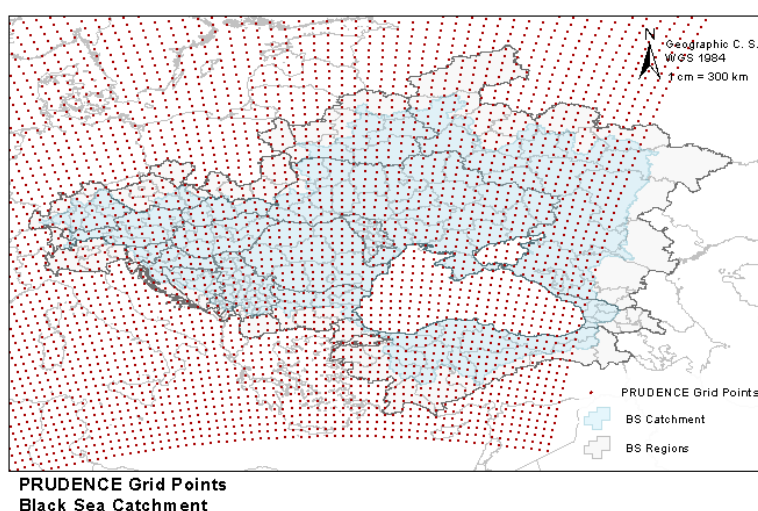
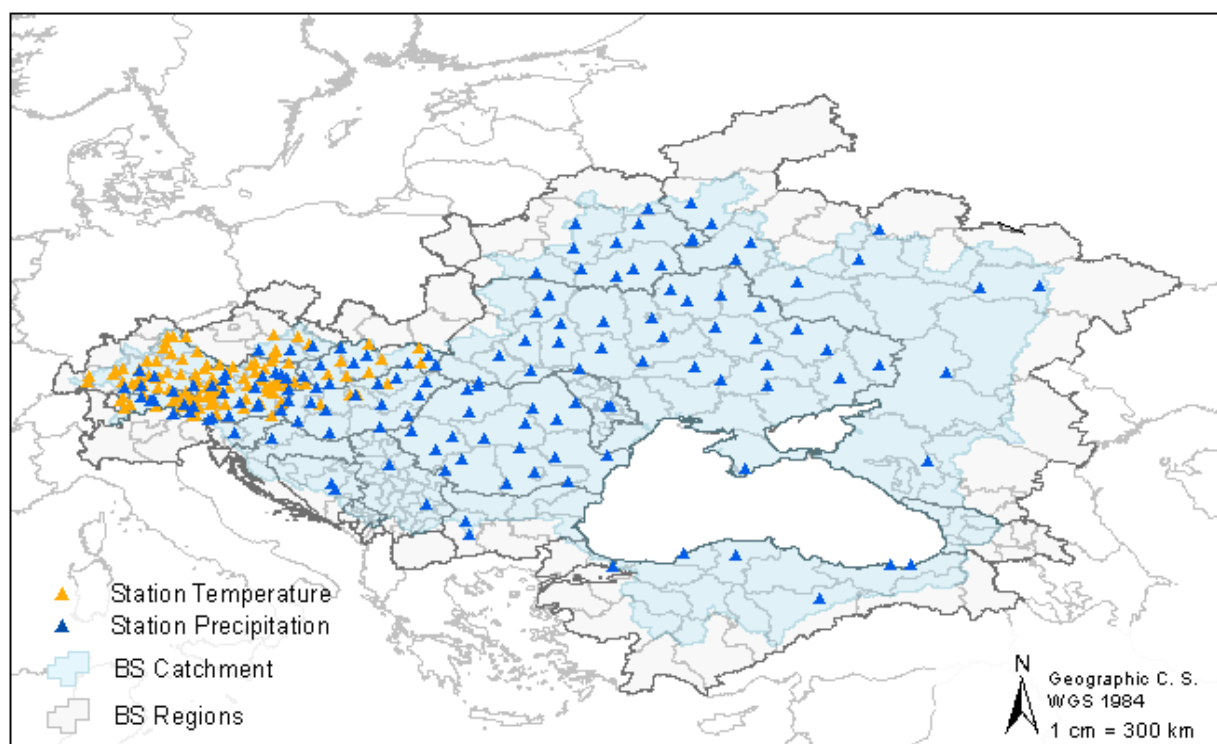


Figure 1 : HIRHAM surface grid mesh – Black Sea catchment

² PRUDENCE: <http://prudence.dmi.dk/>

2.2 Meteorological stations observation datasets

The meteorological observations for precipitation, maximum and minimum temperatures from a subset of 150 Meteorological Stations were provided within the Black Sea catchment. The time frame for these measurements ranges from January 1, 1970 to December 31, 2008, depending on the station. However, large sections of these files contained missing values. This data was provided by Dr. Karim Abbaspour, from the Swiss Federal Institute of Aquatic Science and Technology (Hanganu et al., 2010). The stations with temperature measurements are all located in the western section of the Black Sea catchment, while the stations with Precipitation measurements are dispersed over the Black Sea catchment, as shown in Figure 2.



**Meteorological stations observation datasets
Black Sea Catchment**

Figure 2 : Subset of Meteorological Stations providing observed datasets – Black Sea catchment

2.3 CRU dataset

The CRU is a gridded climate dataset created by the Climate Research Unit (CRU), University of East Anglia (New *et al.*, 1999; New *et al.*, 2000). The different variables were obtained from station observations and the two variables used in this work are part of the primary variables from the CRU monthly grids of terrestrial surfaces climate and were interpolated as a function of latitude, longitude and elevation by the thin-plate splines (New *et al.*, 1999; New *et al.*, 2000).

Since the first version (New *et al.*, 1999), the dataset has been updated with new observations and in addition different datasets are now available for different purposes: climate (New *et al.*, 1999), time-series (New *et al.*, 2000), scenarios (Mitchell *et al.*, 2004), and countries (Mitchell *et al.*, 2002). Both climate and time-series are high-resolution grids, while the climate dataset contains only average values, the time-series contains includes the monthly time-series (New *et al.*, 1999; New *et al.*, 2000). The scenarios were obtained from the combination of the IPCC emission scenarios with four Global Climate Models (Mitchell *et al.*, 2004). The countries dataset aggregates all the above datasets with the addition of socio-economic data (Mitchell *et al.*, 2002).

The dataset used in this work is the CRU TS 3.0, covering the period from 1901 to 2006 with a grid spacing of $0.5^{\circ} \times 0.5^{\circ}$ (CRU, 2008). In this CRU TS 3.0, daily and monthly data are available for cloud cover, diurnal temperature range, frost day frequency, precipitation, daily mean temperature, monthly average daily minimum temperature, monthly average daily maximum temperature, vapor pressure and wet day frequency. Although the Black Sea catchment is covered, the quality of the dataset depends directly on the density of the meteorological stations that were available for the entire time period from 1901 to 2006 (Tapiador *et al.*, 2012).

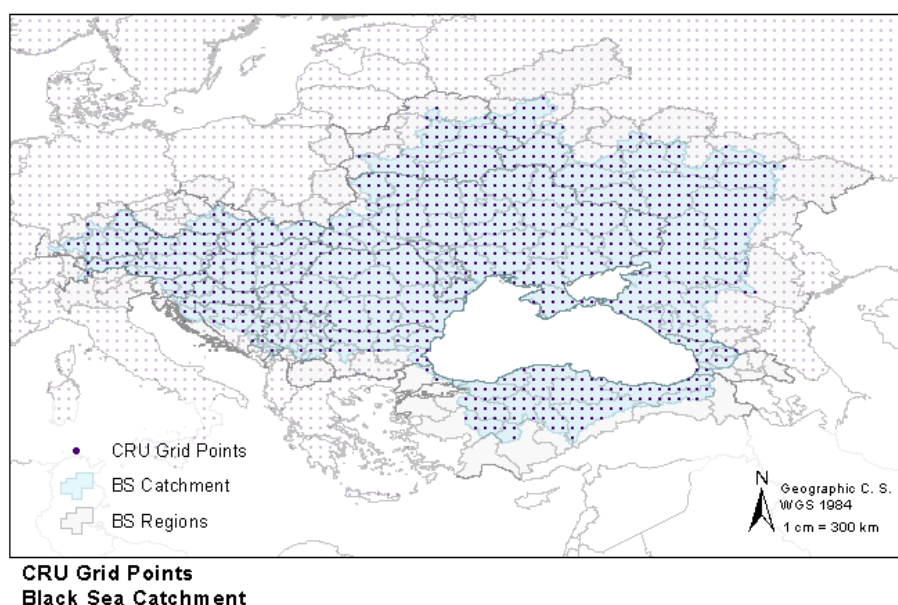


Figure 3 : CRU Grid Points – Black Sea catchment

3 Methodology

Some refinements were made in the application of the “original” DM described in an earlier enviroGRIDS report to temperature and precipitation. Initially, an “annual” version of the DM was used where the daily averages were calculated over the complete year and not separated month by month. The “annual” DM consisted of organizing these daily averages into deciles calculated over the complete year. This resulted in 360 daily averages divided into ten decile categories, while the “monthly” DM results in 30 daily averages divided into ten decile categories, each month stored separately. The latter method allows for an improved accuracy of the results and is therefore the chosen method described in this study.

In addition, running the model on the “annual” DM resulted in a large number of occasions where the “perturbed” T_{\min} on a given day was higher than the “Perturbed” T_{\max} . The “monthly” DM significantly decreased the number of times this result occurred (down to $< 10\%$ of values). In order to correct these errors, an empirical linear relation were derived between both variables. These are highly correlated. Then, all values of “Perturbed” T_{\max} that were lower than the “Perturbed” T_{\min} were replaced by the value issued from this empirical relation. This step was repeated for each “perturbed” weather station, and results in “corrected” meteorological station values.

Two slight changes were made in the DM applied to precipitation; first only wet days were considered. In addition the method was applied to monthly datasets instead of seasonal datasets (DJF, MAM, JJA & SON). The latter change was due to the fact that the results obtained with seasonal datasets showed that much information is lost and it is extremely difficult to automate the choice of a seasonal noise.

The definition of a wet day adopted in this study considers as wet days occurrences when precipitation is more than 1 mm d^{-1} (Ferro *et al.*, 2002; Boberg *et al.*, 2007). All values less than or equal to 1 mm were replaced by missing values (NA); however this threshold can be revised if needed.

In a first step, the perturbation between the HIRHAM control climate (HC1, 1961-1990) and both scenarios A2 (HS1, 2071-2100) and B2 (HB1, 2071-2100) were used to study the applicability of the DM to perturb average values of monthly precipitation. Datasets for daily Pcp, T_{\max} and T_{\min} were downloaded from the PRUDENCE project website for a group of PRUDENCE grid points within the Black Sea catchment area. The selected grid points correspond to the closest grid point to each of the 150 weather stations, in both temperature (Fig. 4) and precipitation (Fig. 5). Some of the grid points were used more than once for different weather stations. Moreover some of the closest PRUDENCE grid points are located outside the Black Sea catchment. The same neighborhood function was applied to the CRU dataset (Fig. 5).

The same methodology was then applied to the HIRHAM simulated precipitation and temperature outputs of the A2 and B2 GHG emission scenario, on observations of the Meteorological Stations in the Black Sea catchment. The available dataset covers a period spanning 01/01/1970 to 31/12/2008. In order to apply the DM under similar conditions, only a 30 years time period was used, i.e., ranging from 01/01/1976 to 31/12/2005.

The DM was implemented using R language for statistical computing (R, 2008) and the final scenarios downscaled to the Meteorological Stations' and CRU Grid points level were exported according to SWAT format requirements. The code can be obtained upon request to the main contributors.

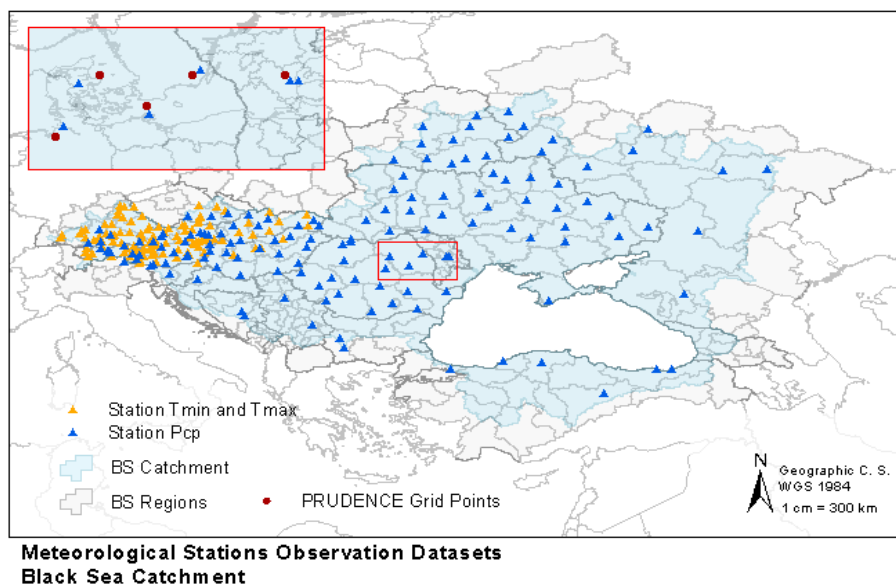


Figure 4 : Closest HIRHAM grid points to a subset of meteorological stations observations datasets

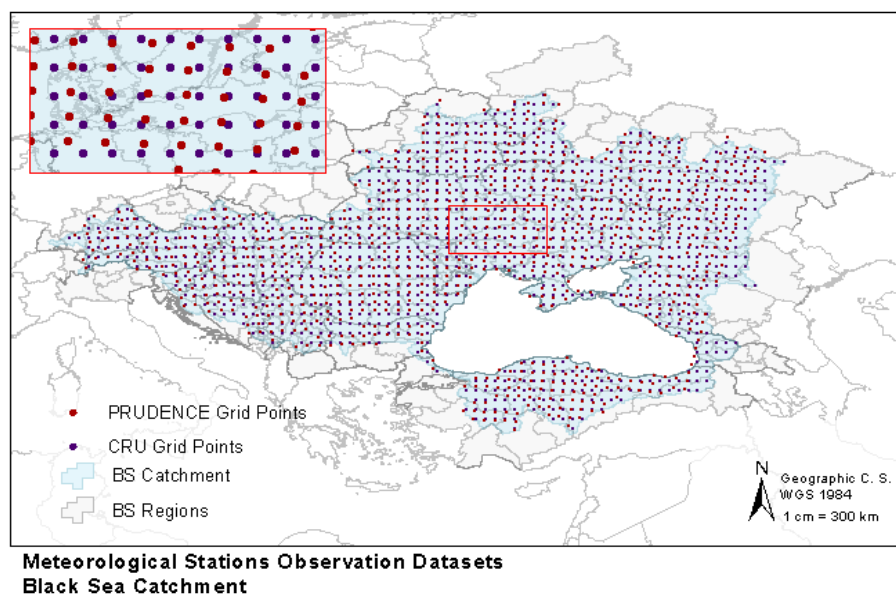


Figure 5: Closest PRUDENCE grid points to the CRU grid points selected for the Black Sea catchment

3.1 Temperature

The methodology applied to the T_{\max} and T_{\min} was divided into two main steps: evaluation of the “deltas” and their application to predictions.

The HIRHAM daily outputs serve to calculate the daily average of the DM for each date of the complete 30-year period, for example calculating the average value of simulated T_{\max} for every 1st of January of the 30-year Control period. In the R software, a loop is developed over the value of each day of the year to calculate its mean value. For each month, the daily averages of each scenario period are then subtracted to the corresponding daily averages of the control period. The daily averages of the control period are then divided into deciles, and the value of each daily average is categorized in its corresponding monthly decile category. This calculation is repeated for each climate scenario of simulated T_{\max} , T_{\min} , and for each month.

The output of this first step of the delta function is a data frame containing the median and standard deviation values for each decile category, for each scenario of each variable, month by month. These two basic values help determine the central and dispersion values of the distribution and are used to calculate the “Perturbed” T_{\min} and T_{\max} values in the prediction function.

The prediction function is the next step of the DM. As the RCM data contains "regular" dates (30 days for each month), an object was created in order to transform the Stations' observations, which are dated according to the Gregorian calendar, into regular dates corresponding to 1st of January 1976 until the 30th of December 2005, as previously explained.

The remaining missing values are then replaced by using a sample corresponding to the same date. In other words, if the value for the 1st of January 1976 was missing, then it was replaced by the existing value of the 1st of January from another year. The missing values for the 29th and 30th February are replaced respectively by the value of the 28th of February or the 1st of March of the same year.

The next step in the prediction function was to calculate the decile categories for each month. Unlike in the delta function, the decile categories are calculated over the complete monthly distributions, and not on the daily averages. In order to reproduce some stochastic variability, a random factor between 1 and -1 was introduced. This value was modified in order to follow a normal distribution, with most values close to 0, and fewer near the extremes of 1 and -1. This random factor was later used in the calculation of the “perturbed” temperature values.

The final step of the prediction function calculates the “Perturbed” T_{\min} and T_{\max} . An incremental value was introduced, whose objective was to increase the magnitude of the perturbation year by year. This incremental value begins at 16/110 (or 0.145), because the altered Station observations being in 1976, and the modeled results begin in 1991 and end in 2100. This increase factor therefore ends at 126/110 (or 1.145).



A random year from the altered station observations was selected, and the “perturbed” values were calculated according to the equation presented in the previous Deliverable. The equation first selects the altered station observations from its first decile category, and adds a factor combining the incremental value, the median of the corresponding decile category from the output of the delta function, the random factor and standard deviation of the corresponding decile category.

3.2 Precipitation

The implementation of the DM for the precipitation was divided into two steps and two R scripts; the first one consists on computing the perturbation on the basis of the PRUDENCE control, HS1 and HB1 scenarios and was named “Perturbation”. The second step (and script) was named “Downscaling” and applies the DM to the meteorological observations.

For the precipitation data of each grid point (Figure 2) for each scenario nine percentiles were determined, in order to have a good overview of the distribution of the values per month. At the same time each percentile was used to obtain a ratio between each scenario (HS1, HB1) and the control period (HC1). The latter allows us to perturb each wet day according to the ratio calculated for the percentile into which it belongs.

For each grid point of each scenario HC1, HS1 and HB1 (Fig. 1) the monthly 5th, 10th, 20th, 30th, 40th, 50th, 60th, 75th and 90th percentiles were obtained, followed by the calculation of the monthly ratio of percentiles between control and future scenarios, that are designated as “preliminary deltas”.

The “preliminary deltas” were applied to the values of the control scenario (HC1) based upon the following rules:

$$\text{if } HC1_{month} < 5^{th} \text{ Percentile} \rightarrow \text{Predicted HS1} = HC1 * 5^{th} \text{ ratio } HS_{month}$$

$$\text{if } HC1_{month} \geq 5^{th} \text{ Percentile} \cap HC1_{month} > 10^{th} \text{ Percentile} \rightarrow \text{Predicted HS1} = HC1 * 10^{th} \text{ ratio } HS_{month}$$

$$\text{if } HC1_{month} \geq 10^{th} \text{ Percentile} \cap HC1_{month} > 20^{th} \text{ Percentile} \rightarrow \text{Predicted HS1} = HC1 * 20^{th} \text{ ratio } HS_{month}$$

$$\text{if } HC1_{month} \geq 20^{th} \text{ Percentile} \cap HC1_{month} > 30^{th} \text{ Percentile} \rightarrow \text{Predicted HS1} = HC1 * 30^{th} \text{ ratio } HS_{month}$$

$$\text{if } HC1_{month} \geq 30^{th} \text{ Percentile} \cap HC1_{month} > 40^{th} \text{ Percentile} \rightarrow \text{Predicted HS1} = HC1 * 40^{th} \text{ ratio } HS_{month}$$

$$\text{if } HC1_{month} \geq 40^{th} \text{ Percentile} \cap HC1_{month} > 50^{th} \text{ Percentile} \rightarrow \text{Predicted HS1} = HC1 * 50^{th} \text{ ratio } HS_{month}$$

$$\text{if } HC1_{month} \geq 50^{th} \text{ Percentile} \cap HC1_{month} > 60^{th} \text{ Percentile} \rightarrow \text{Predicted HS1} = HC1 * 60^{th} \text{ ratio } HS_{month}$$

$$\text{if } HC1_{month} \geq 60^{th} \text{ Percentile} \cap HC1_{month} > 75^{th} \text{ Percentile} \rightarrow \text{Predicted HS1} = HC1 * 75^{th} \text{ ratio } HS_{month}$$

$$\text{if } HC1_{month} \geq 75^{th} \text{ Percentile} \cap HC1_{month} > 90^{th} \text{ Percentile} \rightarrow \text{Predicted HS1} = HC1 * 90^{th} \text{ ratio } HS_{month}$$

$$\text{if } HC1_{month} \geq 90^{th} \text{ Percentile} \rightarrow \text{Predicted HS1} = HC1 * \text{Random}(0 - 1)_{month}$$

The values obtained with the previous calculation are adjusted considering the average ratio of the actual values to the perturbed precipitation values of each month. This value, represents the monthly change, is then applied in the previous equation.

The application of the DM to the meteorological observations follows this step. However, two factors need to be taken into account, the perturbation intensity of the future scenarios and the leap years.

“Future” values of precipitation will take into account the increase of the intensity of the perturbation with time, which scales linearly with the number of days that passed from the first day of prediction:

$$perturbation\ intensity = \frac{\text{u mber of Days that occur from } 3 \text{ } 2 \text{ to the Prediction Date}}{\text{u mber of Days that occur from } 3 \text{ } 2 \text{ to } 3 \text{ } 2 \text{ } 20}$$

The perturbation values obtained vary between 0.85 in the first day of the prediction (01/01/2071) to 1.13 in the last day of the prediction (31/12/2100), while the perturbation is equal to one between 1976 and 1986.

When creating scenario projections for the Meteorological Stations we are working with two time series with bissextile years for a period of 30 years in the past and in the future, which need to be aligned to warrant timing. This issue was overcome by excluding from the existent bissextile years the 29th of February, from the local observations time series and “future” dates. Afterwards, extra days in bissextile years were inserted with A value.

Similar to what was done to extreme values for the estimation of HS1 and HC1 by means of perturbation of HC , extreme values (precipitation values \geq 0th percentile) will be multiplied by a random value between 0 and 1.

4 Results

The following sections provide an overview of the results obtained for both temperature (T_{\max} and T_{\min}) and precipitation (P_{cp}). For each observation, different meteorological stations were selected to show the accuracy of the method. Due to the vast amount of data in the spatial domain, only one station for temperature was retained, whereas for precipitation two different stations were chosen. Afterwards, the results obtained from the DM applied to the CRU datasets are described, by using the observed temperature and precipitation at the closest CRU grid point.

4.1 Meteorological Stations

4.1.1 Temperature

The following figures present various characteristics of the input data used during this study as well as for the predicted temperatures generated by the monthly DM. All figures present the data corresponding to the randomly-picked meteorological station (ID 112700) and associated HIRHAM grid point ID ($i=30, j=44$) located in Austria.

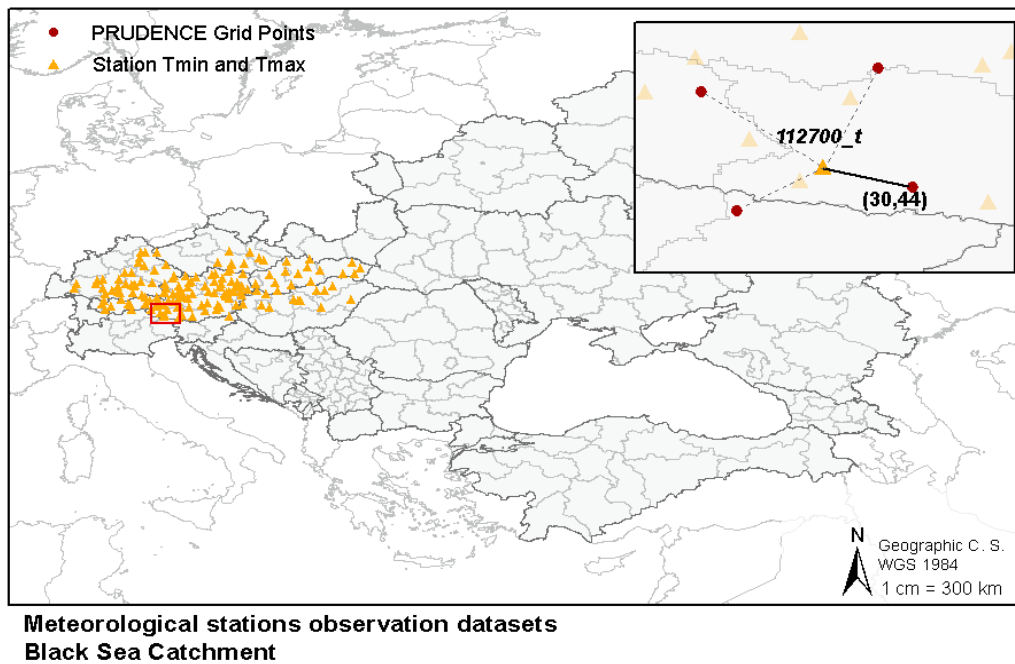


Figure 6: T_{\max} and T_{\min} measured at meteorological station in Austria

As can be seen in [Figure 7](#), the HIRHAM averaged daily values for T_{\min} and T_{\max} create a relatively smooth curve with a seasonal variation of a maximum of 20°C for T_{\max} and 15°C for T_{\min} . It is to be noticed that both A1 and B2 GHG emission scenarios provide higher average temperatures than the control period. The temperatures predicted using the DM present a distribution with much more variation. There is more fluctuation over the averaged daily values, and a larger seasonal variation. The predicted temperatures follow the meteorological station distribution for observed temperatures. The temperature change between the different periods and scenarios are similar to those in the HIRHAM simulated outputs.

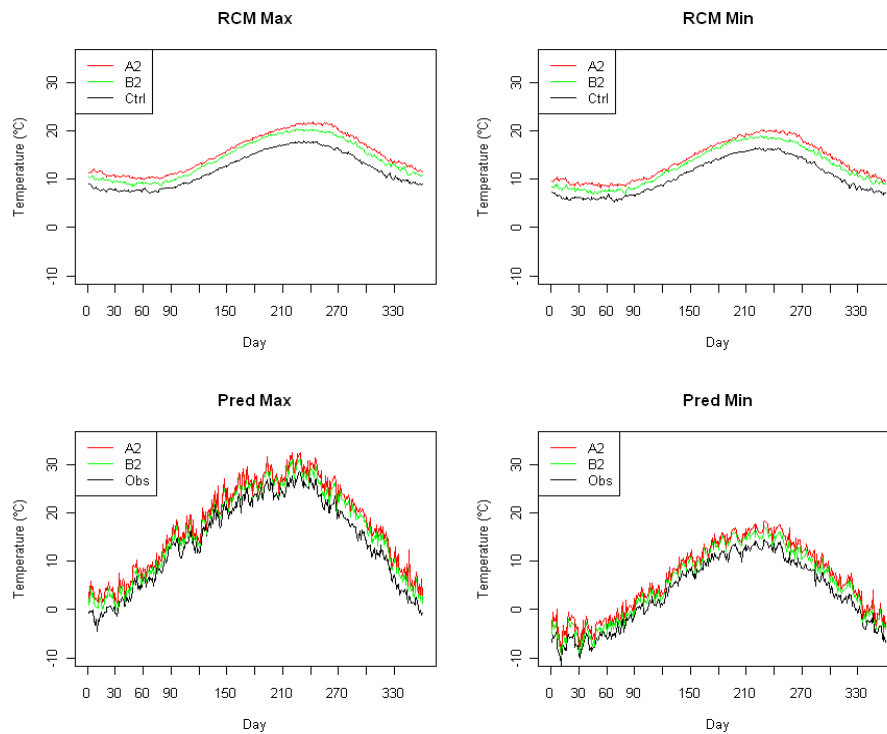


Figure 7 : Averaged daily temperature distributions for weather station ID 112700 and associated HIRHAM RCM grid point Grid point ID (long=30, lat=44) located in Austria.

The annual frequency distributions of the various data that was provided for both observed and simulated T_{\min} and T_{\max} and the future prediction of these, as shown in Figures 9 to 11, all present a bimodal distribution. The HIRHAM frequency distributions show a higher frequency peak at the lower temperature ranges for both T_{\min} and T_{\max} , while the observed distributions provide a slightly higher frequency peak at the higher temperature ranges. The predicted frequency distributions however show that the minimum temperatures reach their highest frequency peak at the lower first mode, while the maximum temperatures reach theirs at the higher second mode.

It is apparent that values simulated with the HIRHAM RCM have a much smaller range than the observed time-series. This suggests that the RCM data does not reproduce accurately the temperature extremes over this location.

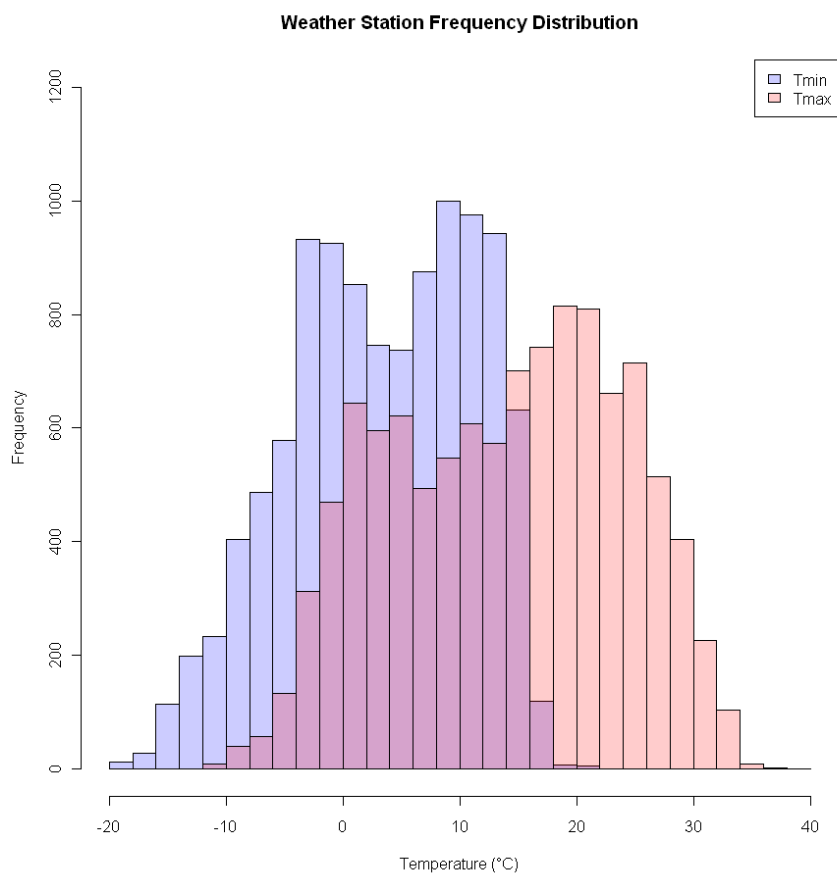


Figure 8: Frequency distributions of observed T_{min} and T_{max} for meteorological station ID 112700 (1976-2005).

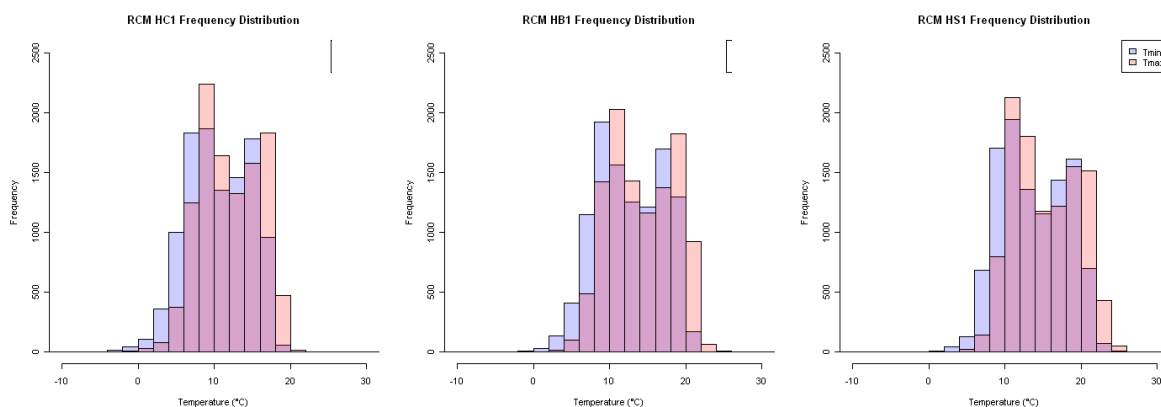


Figure 9: Frequency distributions of simulated T_{min} and T_{max} for HIRHAM grid point (long=30, rlat=44), during the control period (HC1 – 1961-1990) and both SRES scenarios, HB1 (B2) and HS1 (A2) – 2071-2100.

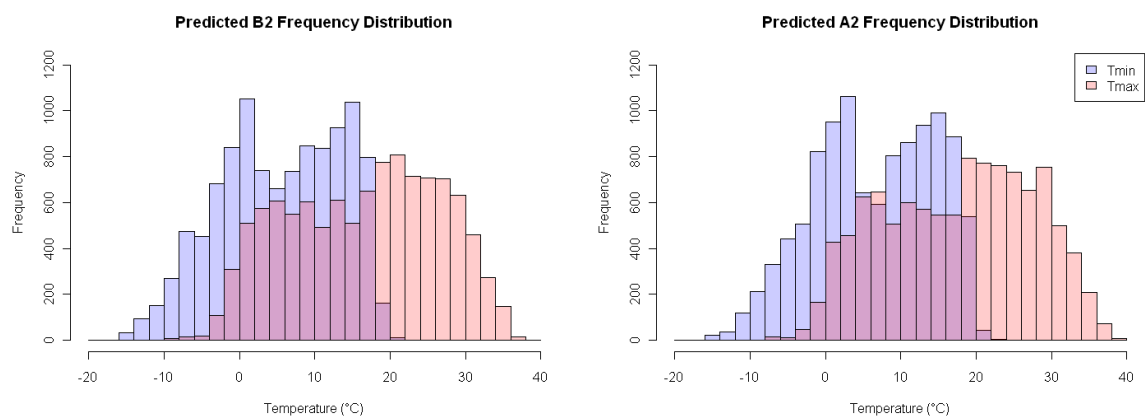


Figure 10: Frequency distributions of predicted T_{min} and T_{max} at Meteorological Station "112700", according to both SRES scenarios HB1 (B2) and HS1 (A2) – 2071-2100.

4.1.2 Precipitation

The validation of the prediction obtained with the DM was made by comparing the monthly average and standard deviation results obtained for both HS1(A2) and HB1(B2) with the original ones. In general the results obtained are encouraging. The average monthly value for the mean and standard deviation for the grid point ID (long=77, lat=24) situated in Crimea, show a clear improvement with the inclusion of the monthly variability, however the results obtained are not completely satisfactory and show that the method needs some improvements:

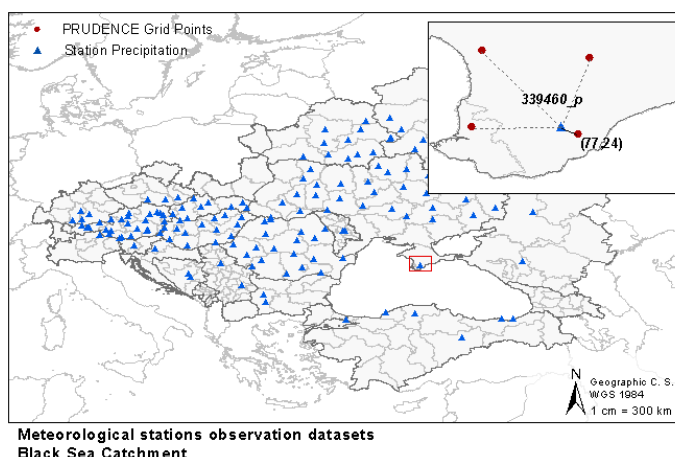


Figure 11: Precipitation Meteorological Station ID 339460_p situated in Crimea

	average	st dev	average	st dev	average	st dev	average	st dev
	HC1		HS1		HS1 - Perturbation		HS1 - Final Results	
January	5.6	6.2	5.9	6.9	4.8	4.5	5.7	4.2
February	6.0	6.3	6.0	6.5	4.9	4.3	6.1	4.9
March	5.9	6.4	5.8	6.5	4.8	4.1	5.5	4.3
April	6.0	6.6	6.2	6.5	5.1	4.4	6.0	4.8
May	6.0	6.4	6.5	7.6	5.1	4.5	6.1	5.4
June	6.0	7.4	6.0	6.4	5.0	4.4	5.8	4.8
July	5.9	5.7	5.9	6.1	5.0	4.5	5.7	4.0
August	6.3	6.9	6.2	7.7	5.2	5.1	6.4	5.7
September	6.9	8.3	5.8	5.6	5.1	4.6	5.8	5.0
October	6.2	6.7	5.7	6.0	4.9	4.4	5.4	4.7
November	6.1	6.5	7.1	8.2	5.5	4.5	6.5	5.3
December	5.4	5.2	6.4	7.8	4.7	3.8	6.0	4.7
	HC1		HB1		HB1 - Perturbation		HB1 - Final Results	
January	5.6	6.2	7.1	7.6	5.8	4.6	8.1	6.0
February	6.0	6.3	5.9	5.9	5.1	4.4	5.7	4.3
March	5.9	6.4	6.4	7.3	5.4	4.5	6.6	5.3
April	6.0	6.6	6.0	6.7	4.9	4.5	5.7	4.6
May	6.0	6.4	6.5	7.9	5.2	5.0	6.1	4.8
June	6.0	7.4	5.6	6.6	4.7	4.3	4.9	5.2
July	5.9	5.7	6.3	6.4	5.1	4.0	6.5	5.1
August	6.3	6.9	6.8	7.5	5.3	4.3	7.2	5.6
September	6.9	8.3	6.9	8.2	5.5	4.8	7.2	6.2
October	6.2	6.7	6.8	8.5	5.5	5.0	7.2	6.2
November	6.1	6.5	6.2	6.5	4.9	4.0	5.4	4.1
December	5.4	5.2	6.9	8.6	5.2	4.4	6.9	5.4
	mm/day	mm/day	mm/day	mm/day	mm/day	mm/day	mm/day	mm/day

Table 1: Averages and standard deviations of control, future scenarios and final results, gridpoint id (lon=77, lat=24). HC1=Control, HS1=A2 and HB1=B2

Figures 12 and 13 give an example on how the predicted values for HS1 and HB1 improved with the inclusion of the monthly variability, for the gridpoint id (i=77, j=24). While figure 14 gives an overview of the frequency distribution for the months of January and April.

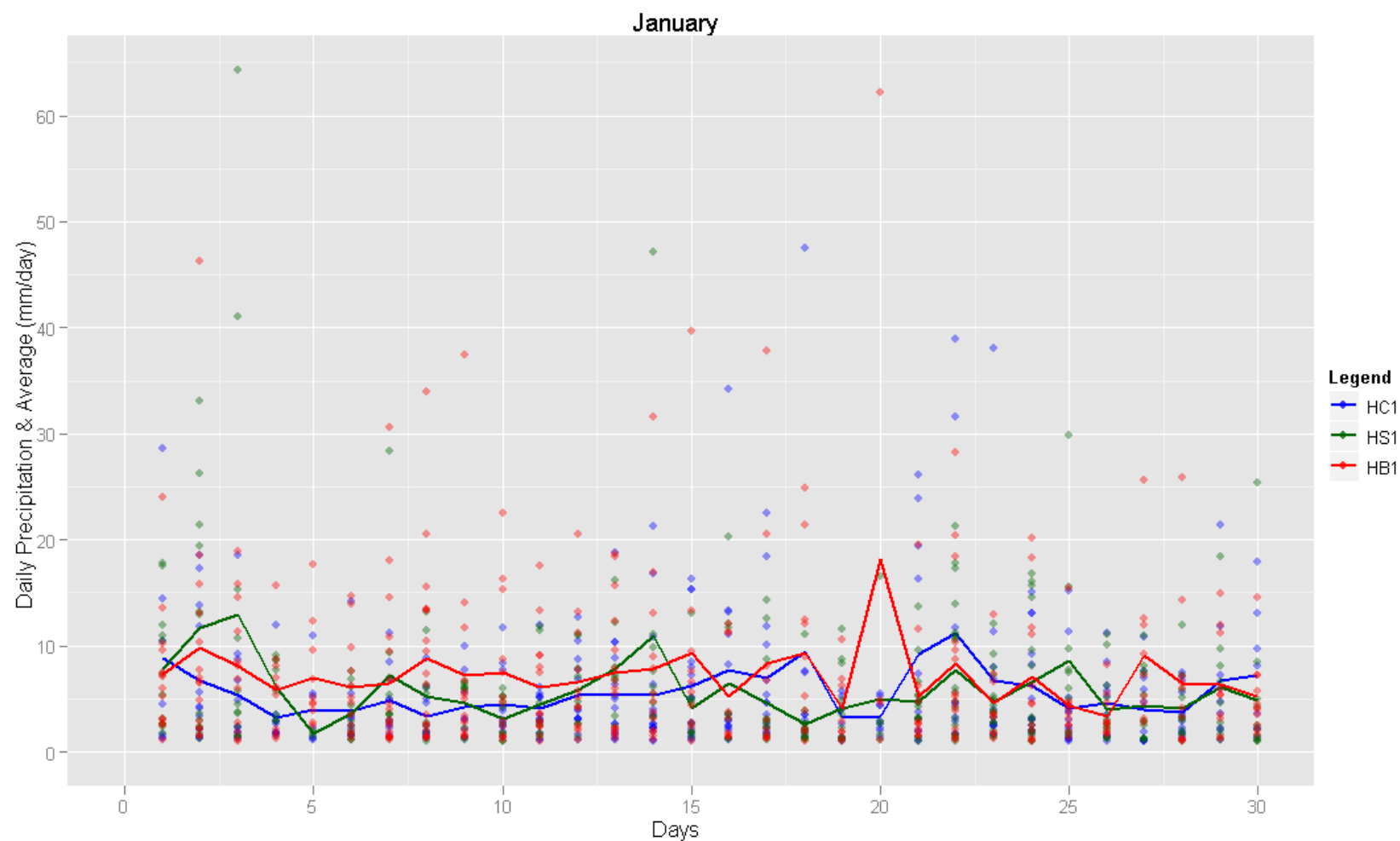


Figure 12: Precipitation values for HC1, HS1 and HB1 PRUDENCE Scenarios, Grid Point ID (lon=77, lat=24)

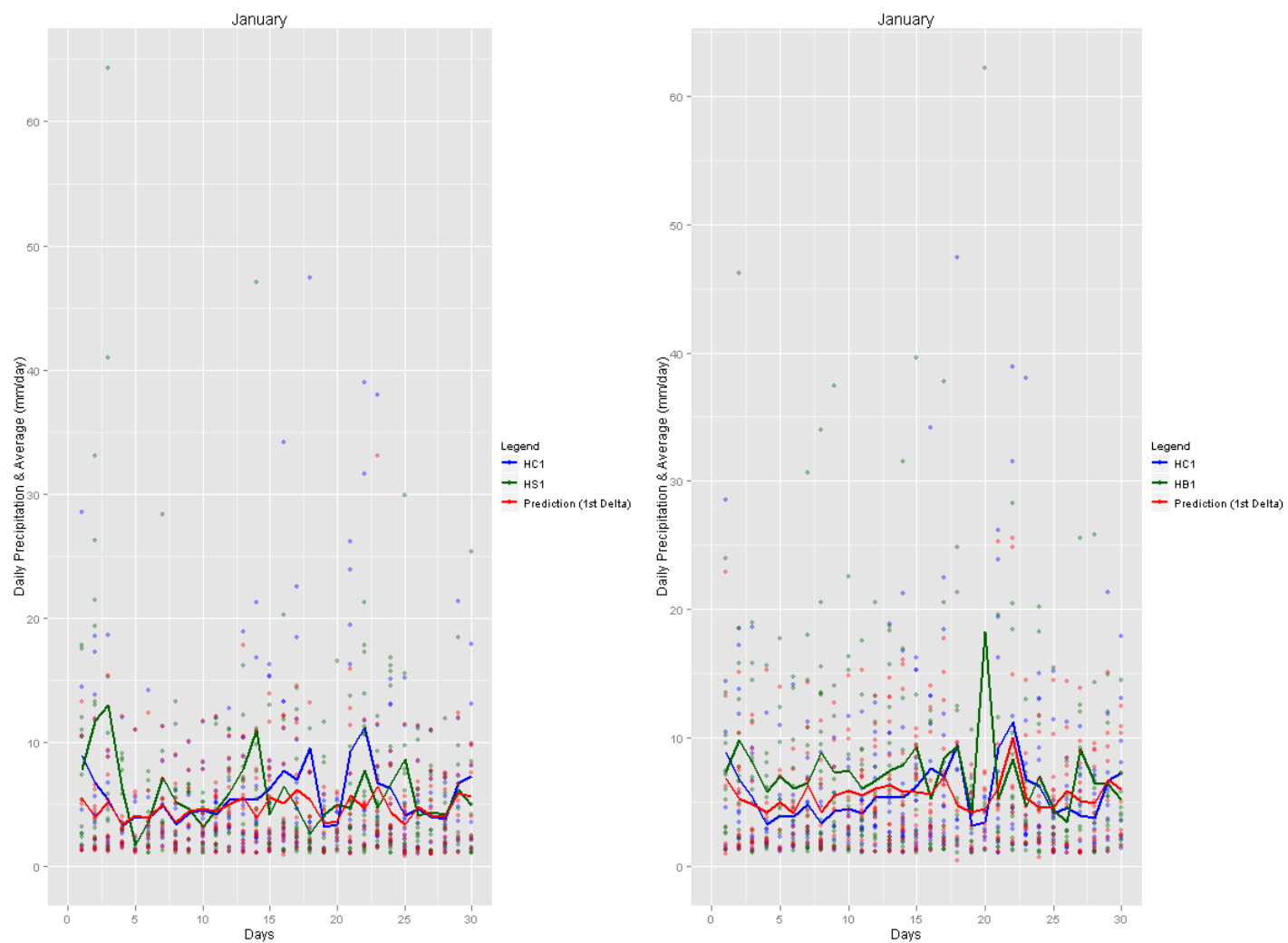


Figure 13: Precipitation values for HC1, HS1 and perturbed HC1 (preliminary perturbation of HC1), Grid Point ID (long,rlat)=(77,24)

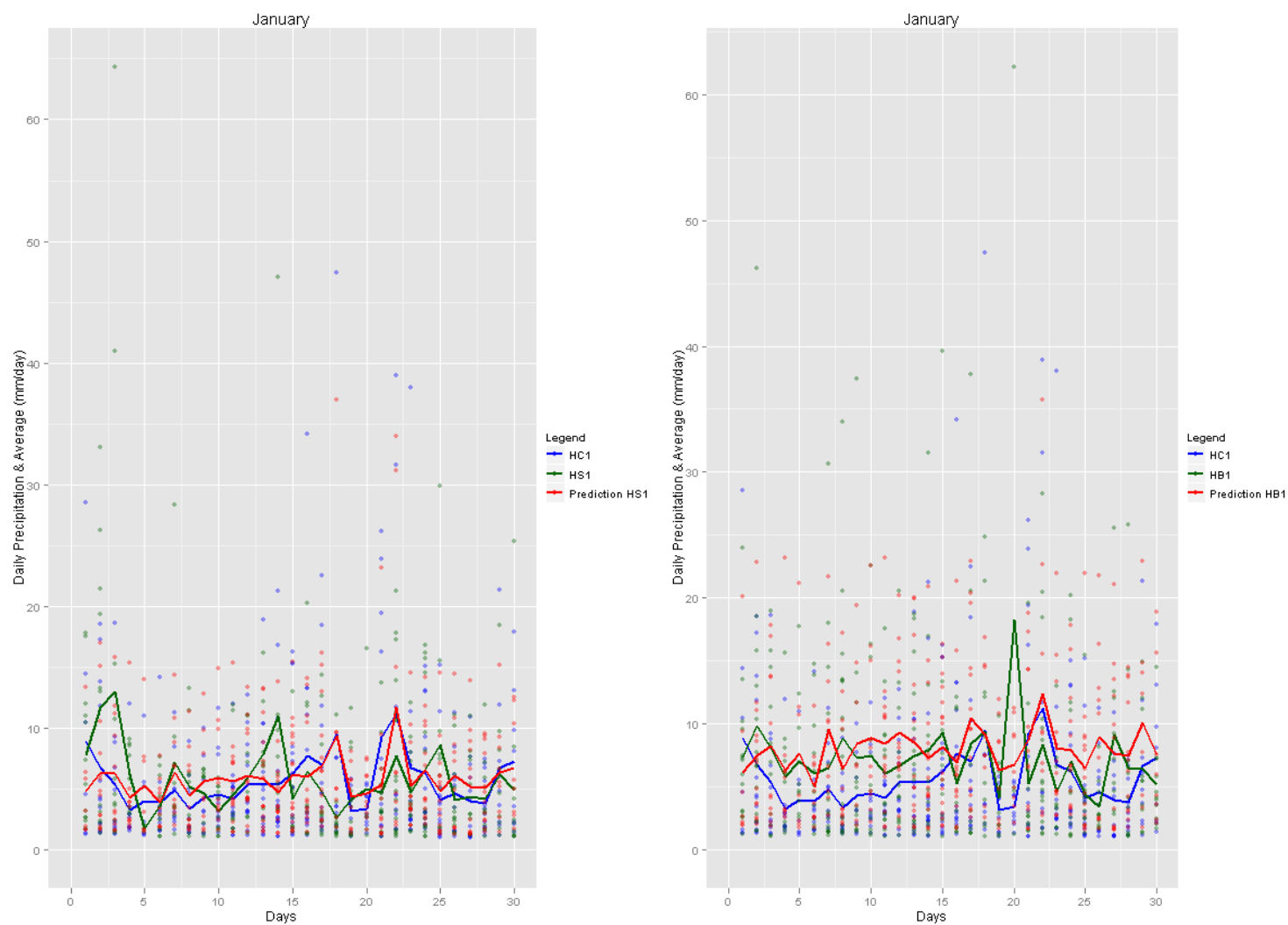


Figure 14: Precipitation values for HC1, HS1 and perturbed HC1 (final perturbation of HC1), Grid Point ID (lon=77, lat=24)

The results obtained for the perturbation of the HIRHAM precipitation show that there is a possibility to correlate the monthly values at model grid points with the observation values from neighboring meteorological stations. As an example, for the results obtained for the closest meteorological station to the selected HIRHAM grid point, the observed *Pcp* at Station 339460_p in Crimea and Station 111650_p in Austria, as well as the results obtained for the scenarios are shown in the following.

When applying the DM to the meteorological stations, the results obtained show that the “future” time series have similar amplitude of precipitation values for these stations, when compared to the observation datasets, a decrease of the number of extreme precipitation values is noticed (Fig. 16 and 18).

With respect to the number of wet days, the results obtained for climate scenario HB1 show a small reduction of the number of wet days (Figure 17 and 19). The strongest difference between observation period and scenarios is obtained with the mean monthly precipitation values. Months with an average precipitation of $> 10\text{mm day}^{-1}$, will decrease in both scenarios. However months with small averages in the observation period, will increase.

The percentile values of the precipitation shown in Figure 15 show a change in the highest percentiles (90%) between the observation period and both scenarios in January, for the meteorological station ID 111650_p and 339460_p.

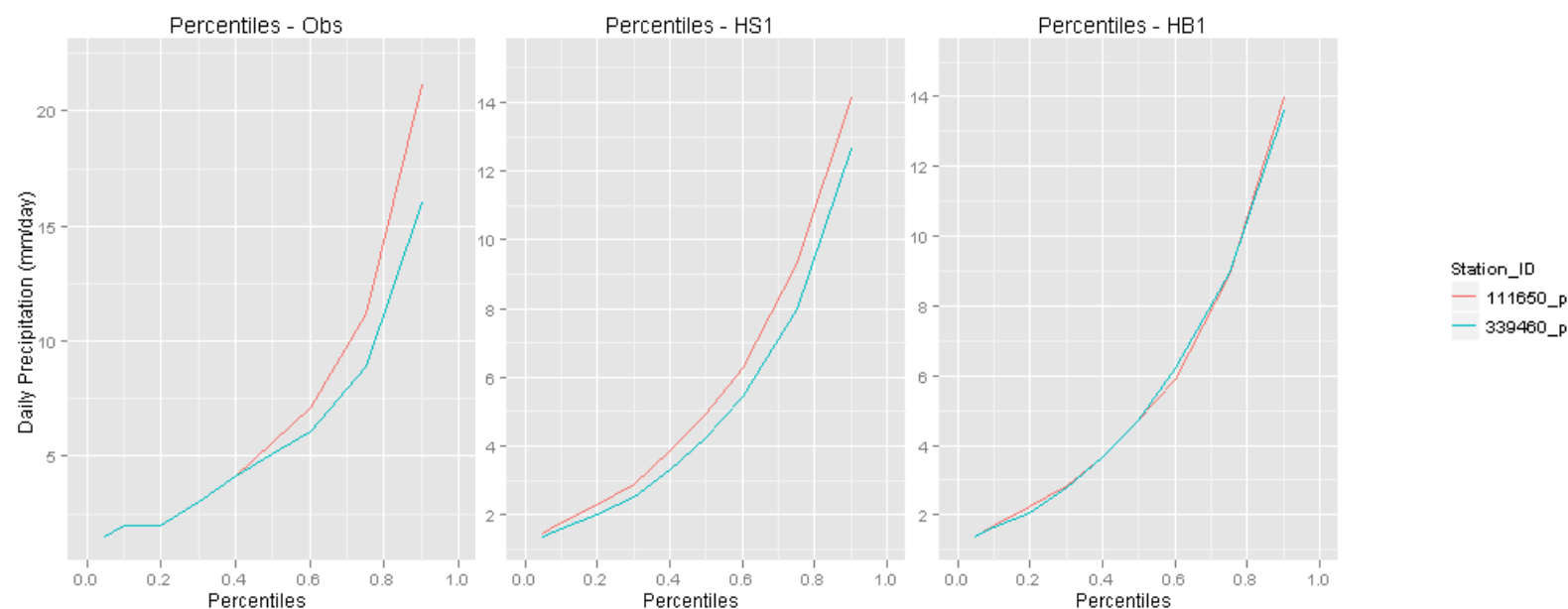


Figure 15: Observations and climate scenarios percentiles: station ID 111650_p and 339460_p

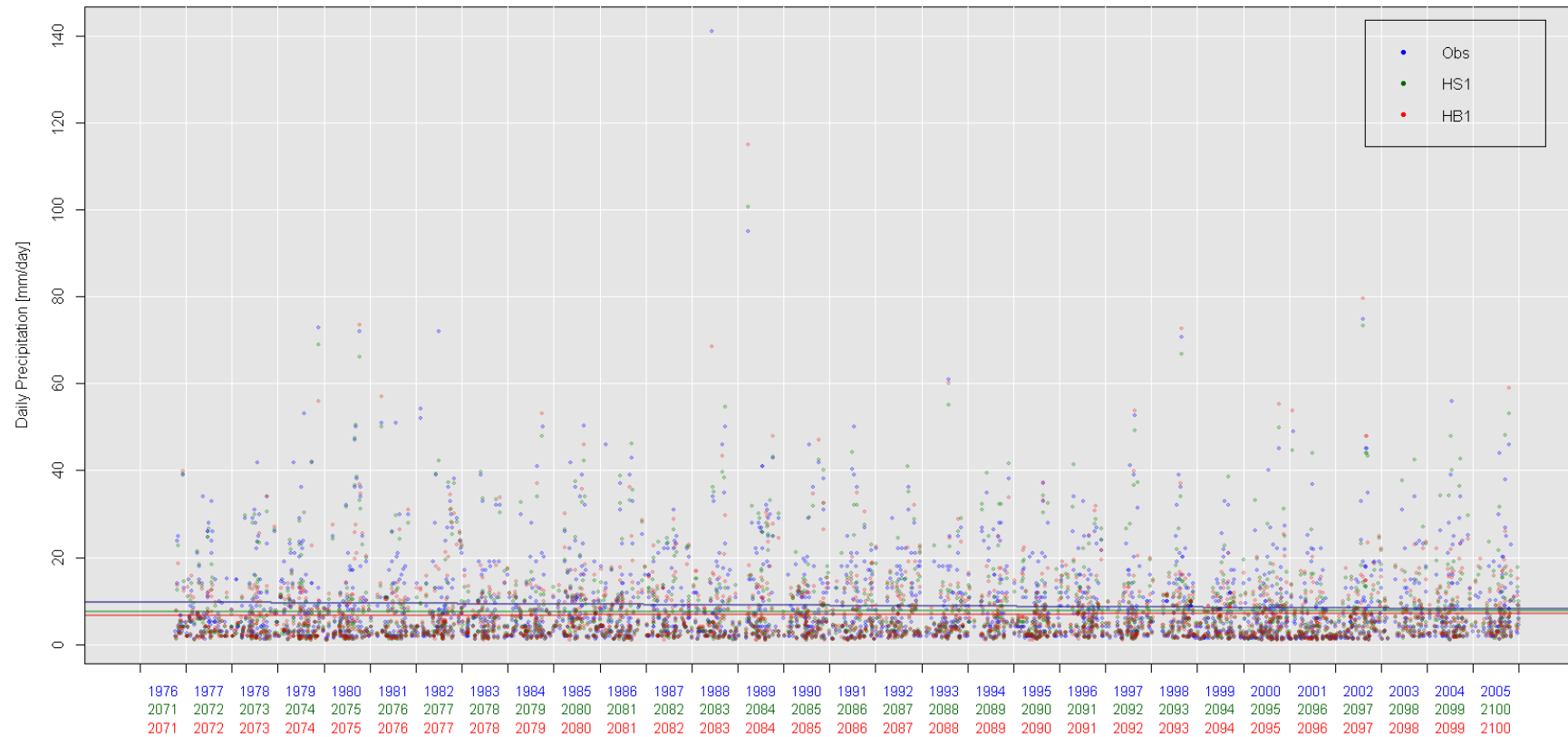


Figure 16: Precipitation time series for station ID 111650_p

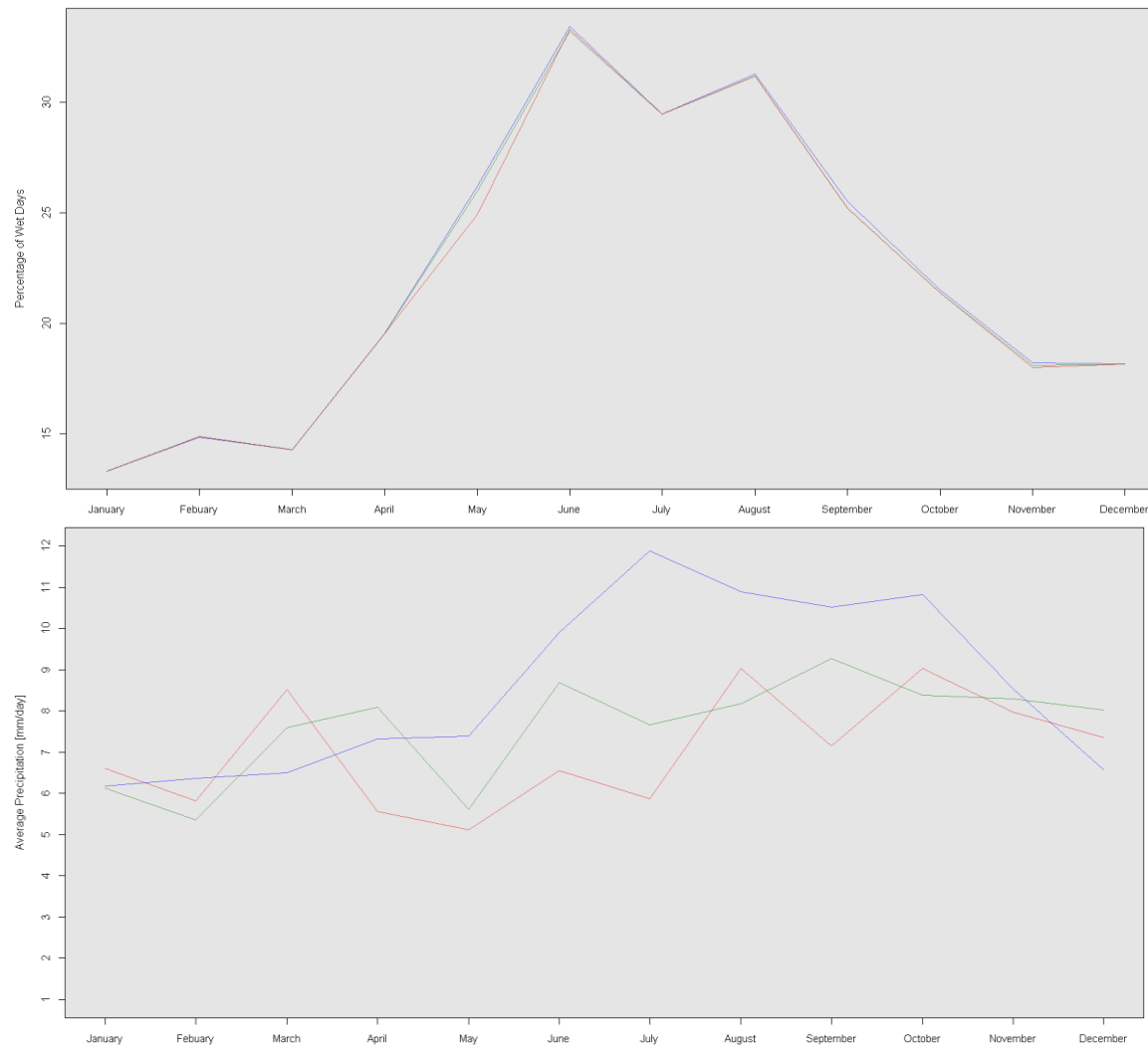


Figure 17: Percentage of Wet Days and Average Monthly Precipitation for Station ID 111650_p

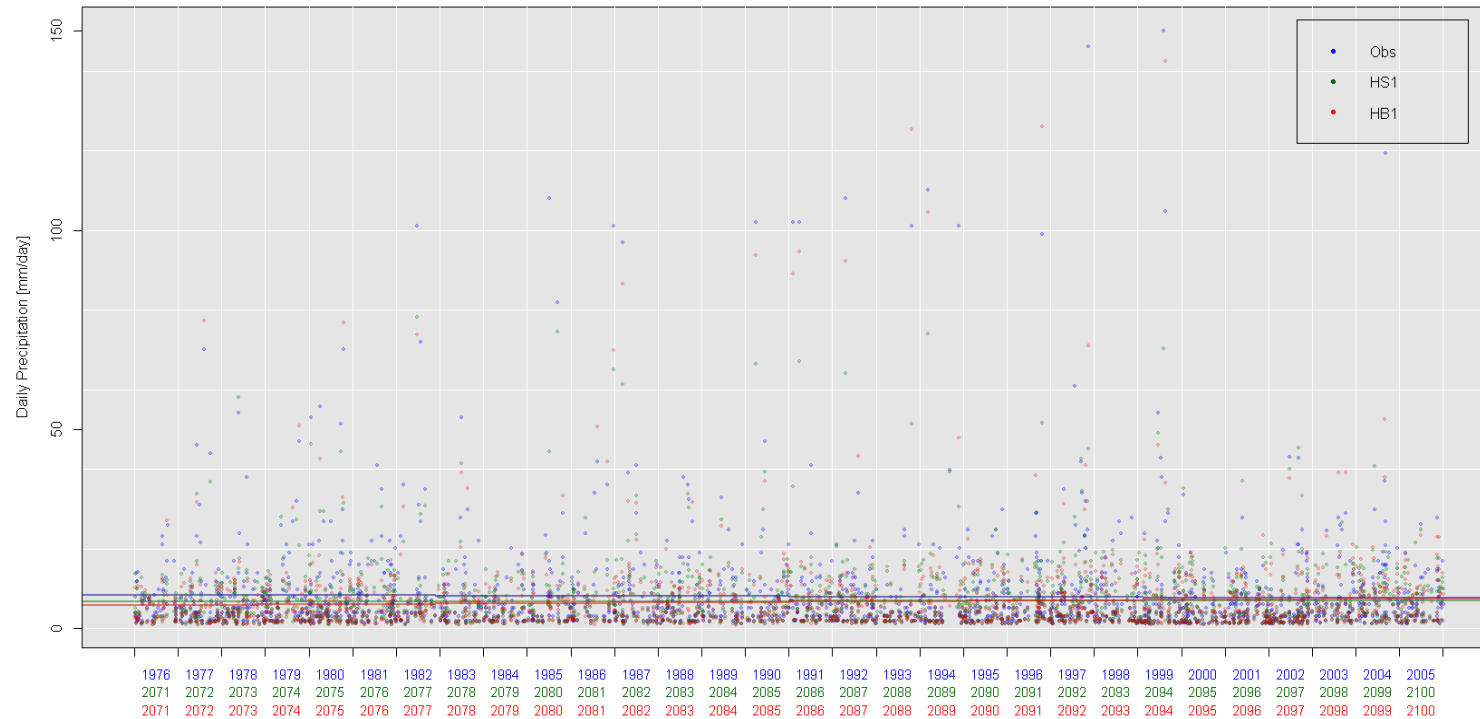


Figure 18: Precipitation time series at meteorological station ID 339460_p

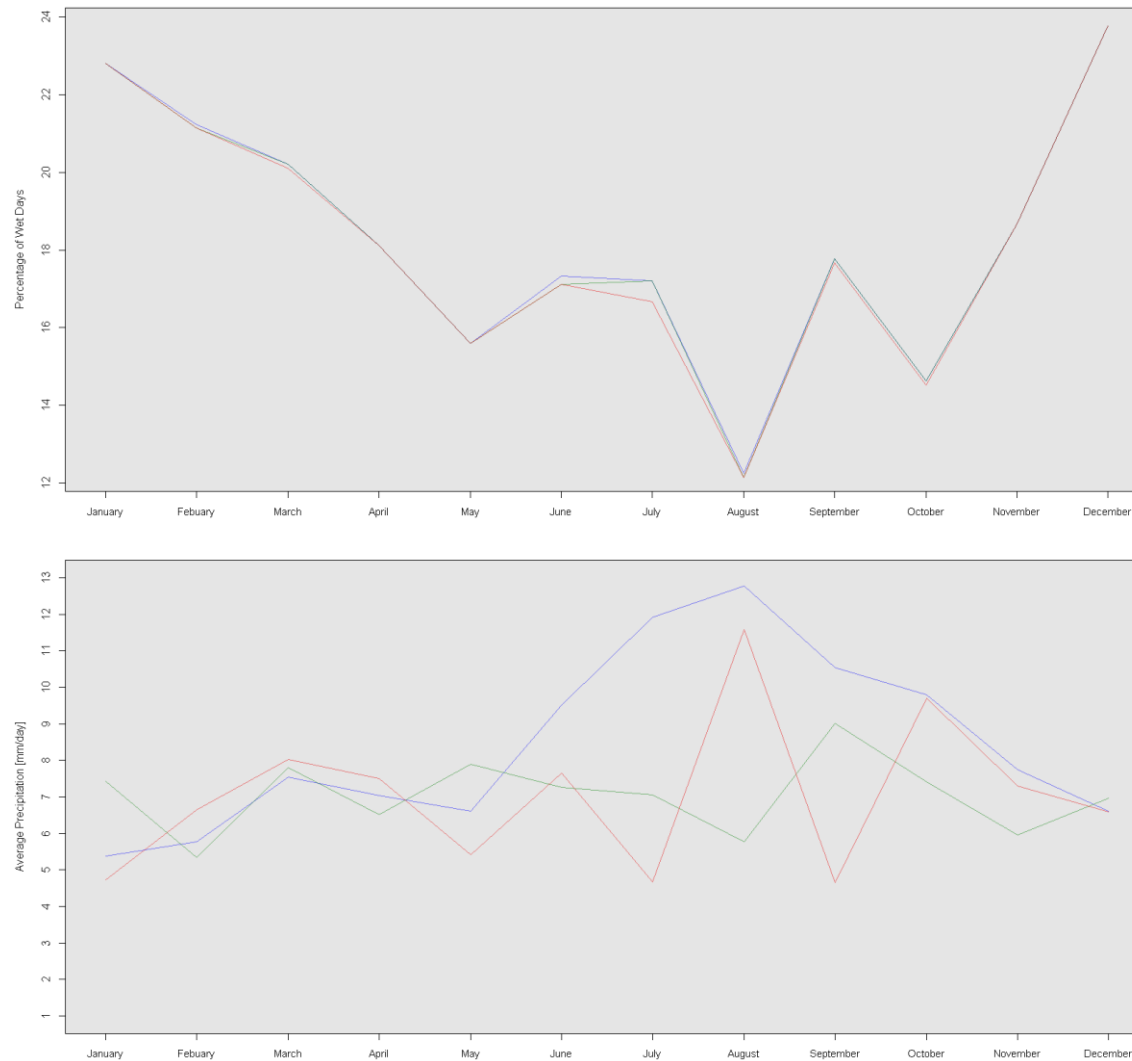
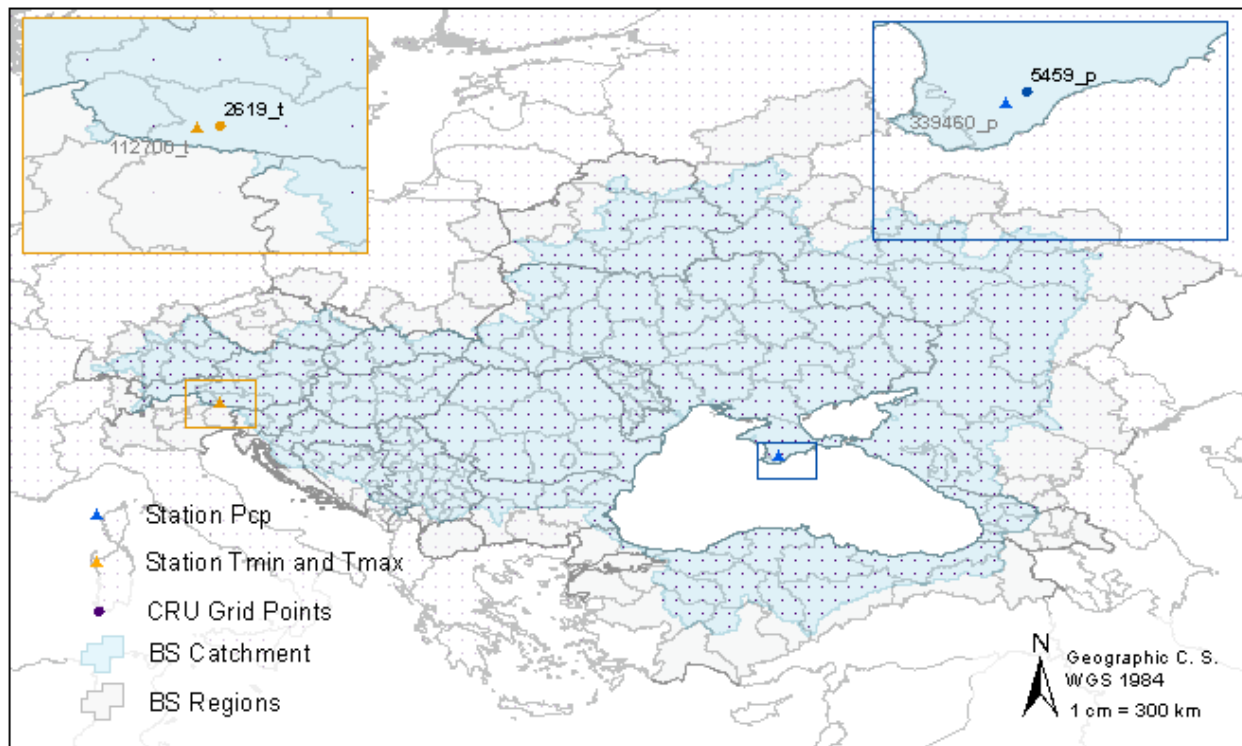


Figure 19: Percentage of Wet Days and Average Monthly Precipitation for Station ID 339460_p

4.2 CRU Dataset

The closest CRU gridpoint to the meteorological station used for temperature (CRU ID 2619_t) and also the closest to one of the meteorological stations used for precipitation (CRU ID 5459_p), were selected to illustrate the result obtained for the DM applied to the CRU dataset. The following figure gives a view of the spatial locations of the selected CRU gridpoints in relation to the respective meteorological station:



**CRU Grid Points
Black Sea Catchment**

Figure 20: CRU gridpoints - Selected gridpoints

4.2.1 Temperature

Figure 21 shows that as it was observed previously with the application of the DM to the meteorological stations, the HIRHAM daily-averaged values for T_{\min} and T_{\max} generates a relatively smooth curve in comparison to the corresponding CRU values. It is to be noticed that the averages of T_{\min} and T_{\max} from the CRU period shows a high variation for the transition between the different months. This behavior will then be transmitted in both climate scenarios. The temperature change between the different periods and scenarios are similar to those in the RCM data.

The frequency distributions of the various data that was provided for both T_{\min} and T_{\max} (observed and simulated temperature values) and the predicted ones, shown in Figure 22, all present bimodal distributions.

While the HIRHAM frequency distributions show a higher frequency peak at lower temperatures for both T_{\min} and T_{\max} , the CRU frequency distributions provide a higher frequency peak at higher temperatures. However the CRU ID point selected shows frequency distribution for both T_{\min} and T_{\max} closer to HIRHAM.

It is also noticeable that both HIRHAM and CRU data have similar range of values for the period, derived also from the “origins” of the CRU dataset.

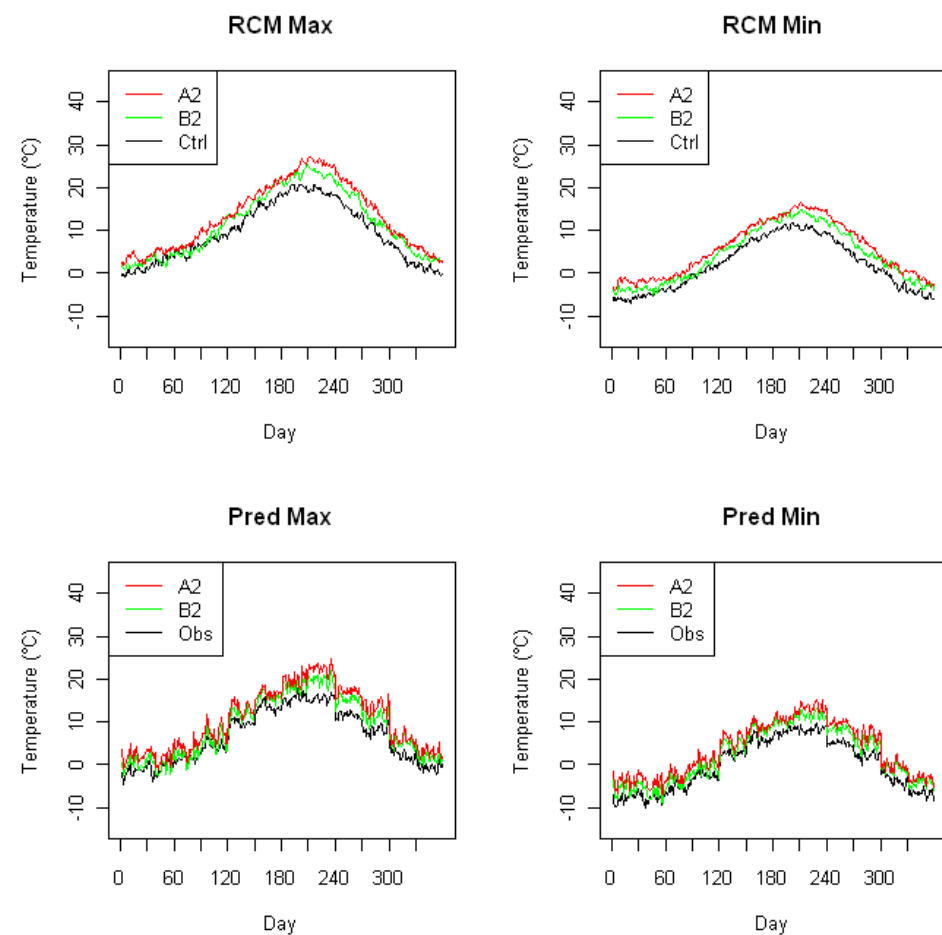


Figure 21: T_{\min} , T_{\max} averages for CRU ID Point 2619_t

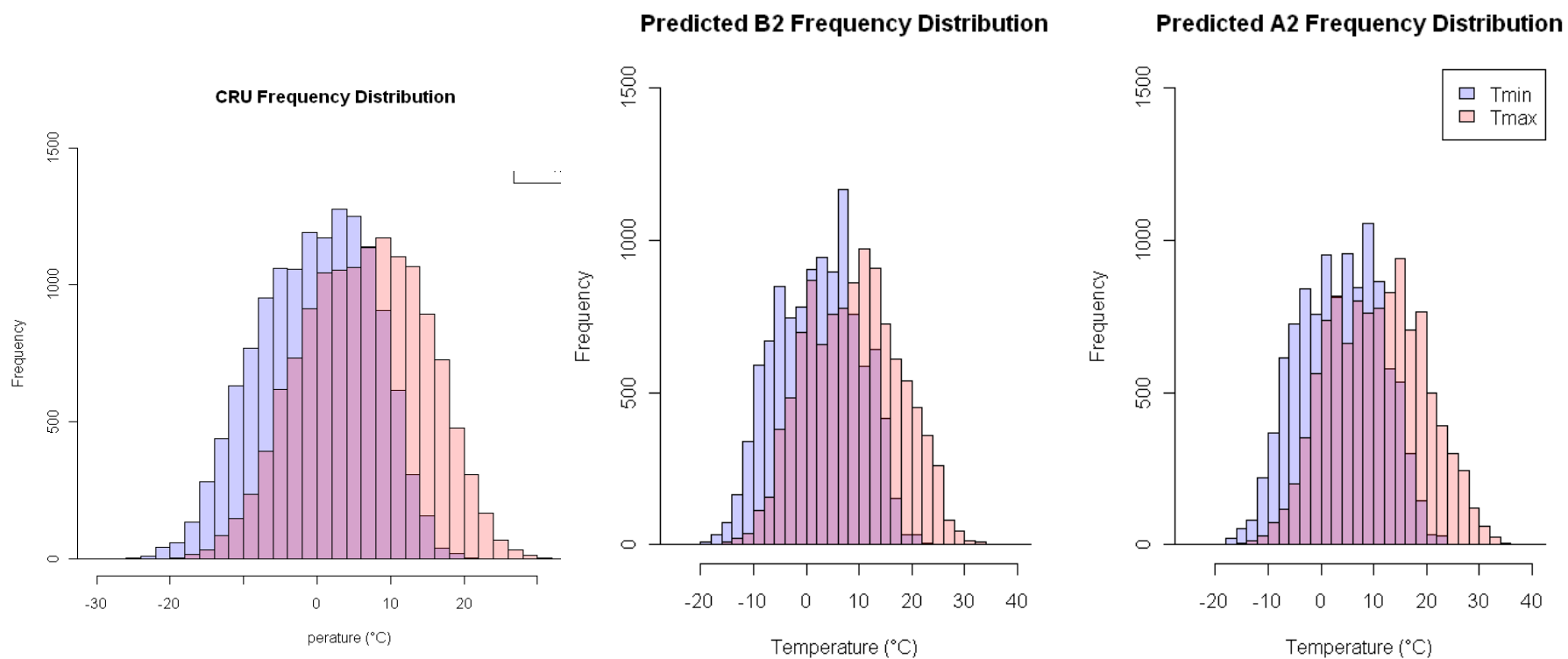


Figure 22: Temperature frequency distribution of Observation period and Predicted scenarios, CRU ID point 2619_t

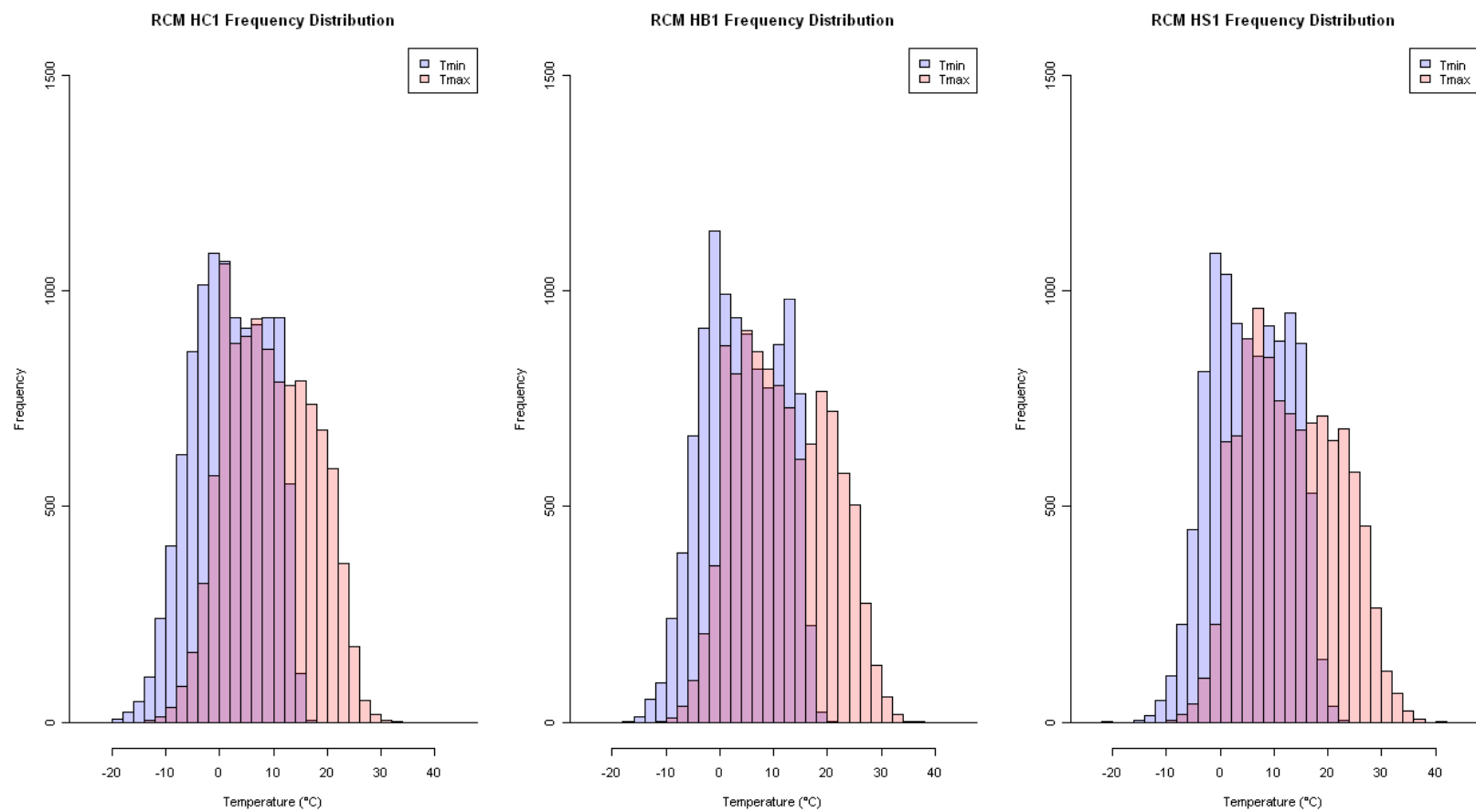


Figure 23: Temperature frequency distribution of PRUDENCE RCM, CRU ID point 2619_t

4.2.2 Precipitation

The precipitation time series of the CRU also shows that the long-term trend for 30 years is similar to the observation period, with a small increase in comparison to the downscaling of HIRHAM climate scenarios to the observed Meteorological Stations ID 339460_p. A decrease of the maximum precipitation values throughout both observed and scenario time series is noticed.

The results obtained for the average fraction of wet days per month in comparison to the results obtained for the meteorological station, show that the months from June to September have a significant difference when compared to the CRU dataset (Fig. 25). Moreover, for the rest of the months, the CRU has a higher fraction of wet days per month over this 30 years period.

Although most of the months have a higher fraction of wet days over this period of 30 years in the CRU dataset, figure 25 shows that the amplitude of the average precipitation per month is smaller when compared to the nearest meteorological station observations and scenarios.

The precipitation percentile distributions in figure 23 show also a change in the highest values (90%) between the observation period and both climate scenarios in January.

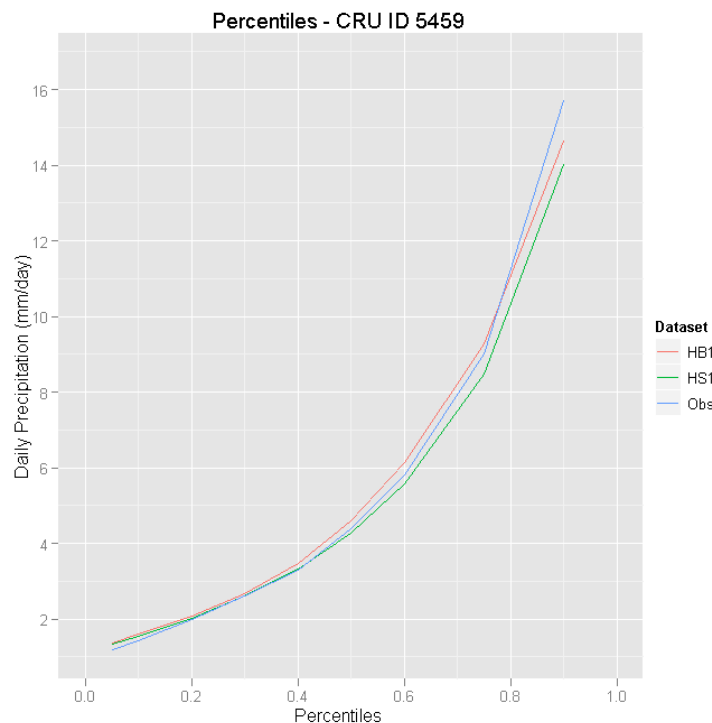


Figure 24 : Precipitation percentiles values for January at CRU point ID 5459_p



Figure 25 : Precipitation time series for CRU point ID 5459_p

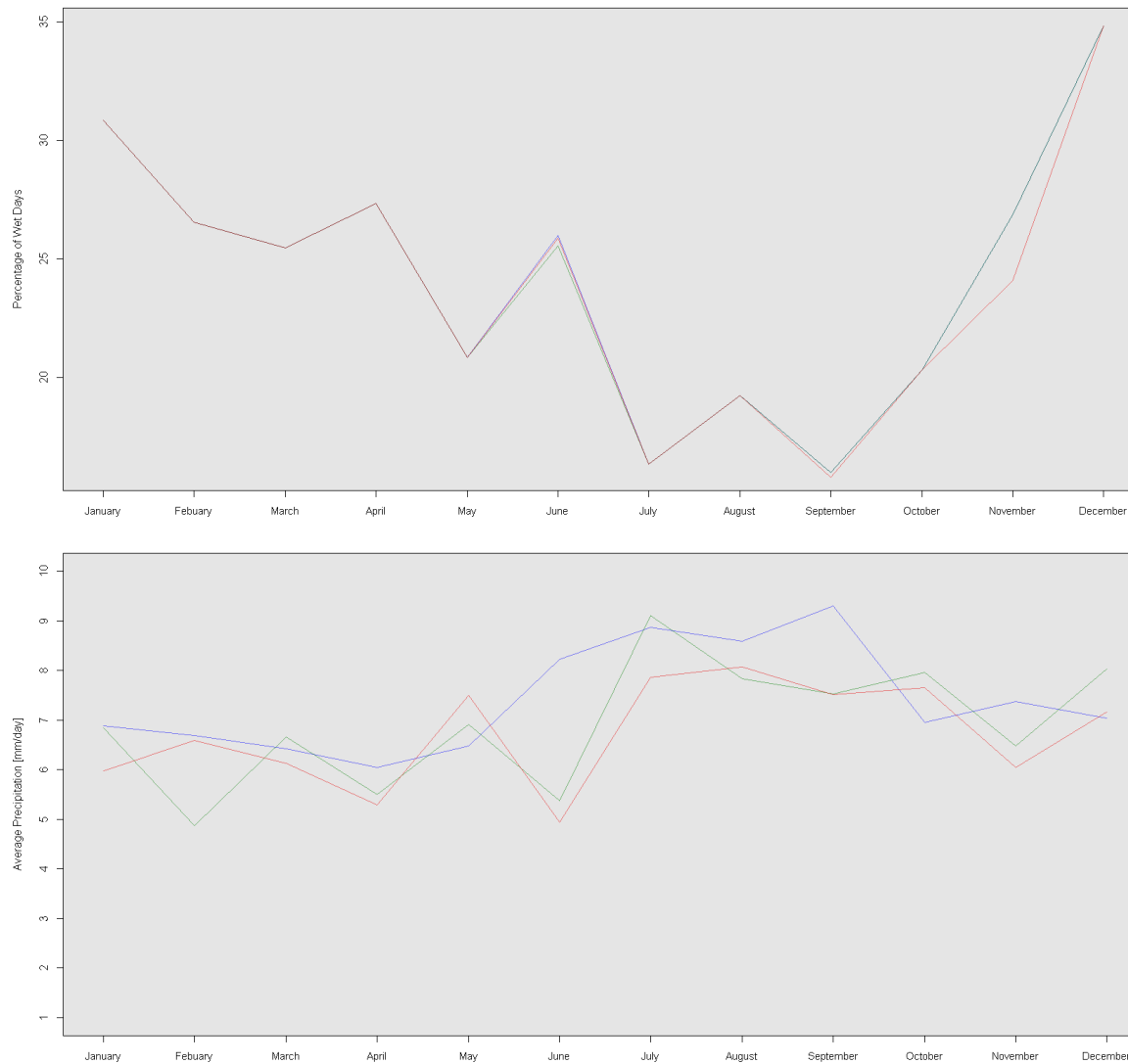


Figure 26: Percentage of wet days and monthly average precipitation at CRU point ID 5459_p

5 Discussion and Conclusion

The results obtained for both meteorological stations and the CRU dataset, show that the predicted minimum and maximum temperatures distributions are close to those observed at the meteorological station and of the CRU values, while taking into account the temperature shift corresponding to the HIRHAM climate simulations. In addition, our assumption that RCMs simulate relative values better than absolute values seems to be valid due to the shorter range of the RCM distributions compared to the observed temperature distributions from weather stations. However the comparison between the observed period of both CRU and closest HIRHAM grid point, suggests that the CRU data does not reproduce accurately both temperature and precipitation. This conclusion is based on the irregularity observed between consecutive months for the temperature in addition to the low magnitude of precipitation values.

The assessment of the CRU dataset is dependent upon the comparison of the observations for the entire Black Sea catchment, for now the meteorological stations with temperature observations are only available for a small area of the catchment, while although precipitation observations are available for the entire catchment, the number of stations is small. A better coverage will be needed to make an adequate assessment. Furthermore, more information concerning the spatial location and the time period of the meteorological stations employed in the interpolation of the CRU climatic grids will allow for a better assessment of the results (Tapiador et al., 2012).

We have found that the DM can give satisfying results for a large time series, when considering the monthly variability. Different studies have reached similar conclusions (Graham et al., 2007; Lenderink et al., 2007; Bosshard et al., 2011). However we must take into account the fact that by using a DM applied to precipitation, extreme values in the past are multiplied by a random number between 0 and 1, resulting in the weakening of the values obtained for “future” observations (Graham et al., 2007). The inclusion of more dedicated perturbation rules for the precipitation extreme values might help to improve this version of the DM (Lenderink et al., 2007). A more recent study shows that the DM can be improved with the inclusion of the climate change signal’s annual cycle (Bosshard et al., 2011).

6 Recommendations for SWAT users

There are significant scientific disagreements over what the best resolution for forecasting the impacts of climate change on water use, agriculture and biodiversity should be. The relatively coarse resolution of GCMs (~200 km) or RCM (~50 km) is simply not practical for assessing water management, where orographic and climatic conditions vary significantly across relatively small distances. Moreover, changes in topography and climate variables are not the only factors accounting for variability in agriculture; soils and socioeconomic drivers, also often differ over small distances, influencing agro-ecosystems, increasing uncertainties, and making forecasting and assessment models more inaccurate and complicated to calibrate.

The Soil and Water Assessment Tool model (SWAT) hydrological model would need optimally input variables such as temperature, precipitation, solar radiation, etc. with the highest spatial resolution possible, as well as covering a sufficient long period of time, in order to warrant realistic energy and water budget to compute accurate budgets within a given catchment. However, such requirements still can't be completely fulfilled, for practical and technical reasons. The mismatch in scales, these resolved by GCM or RCM and these required by hydrological model such as SWAT is still an issue for which many efforts should be devoted.

On simple way to overcome this problem would still eventually suggest using gridded outputs from simulations carried out with weather (NWP) or climate (GCM/RCM) numerical models. However, the spatial resolution of their outputs of temperature, precipitation and other relevant variables is insufficient to drive a hydrological model such as SWAT in order to produce realistic results. The same conclusions can be drawn from gridded observations such as the CRU dataset, or reanalysis data (i.e, NCEP- CAR, ECMWF), where their “low” spatial resolution prevent from using these as inputs in most infra-continental catchment hydrological models.

In order to provide the SWAT users with a method to use the atmospheric variables on the long term, the so-called “delta-method” approach has been devised to extend the length of meteorological records beyond the observed period. This method is based on perturbations (i.e. deltas) that may be derived from either GCMs or RCMs simulated outputs and methodically applied to observed time series. This method has the advantage of using observed meteorological records to drive SWAT over the available observation period so that this model can be calibrated using realistic data; consequently, SWAT outputs can thus be compared and validated against observed water discharge, mineral content, etc. In addition, when the “deltas” are well defined, the observations can be perturbed to “represent” future climate with some confidence, and numerical investigations of the impact a changing climate on hydrology with SWAT can be carried out. The disadvantages of such a technique are that it depends on the density of meteorological stations providing the needed observations and to their length, however. If the catchment under investigation is not densely covered with observation stations, the energy and water budgets may not correspond to the observed ones. The same goes for the length of the observed time series; if the period is not long enough, the inter-annual variability may not be well captured and the climatic conditions over the catchment



and experience some severe biases. Both problems associated with data scarcity (space) and paucity (period) can't be overcome with simple spatial and temporal interpolation techniques. The natural spatial and temporal variability can't be re-injected without any further assumptions nor the development of extra working hypothesis.

Consequently, some “general” recommendations on the use of the DM can be given to the scientific community to drive SWAT over sub-continental catchment, such as the Black Sea catchment:

- Ensure that the catchment has “enough” weather station observations to provide the necessary atmospheric input for SWAT to reproduce the hydrological regime accurately. Note that during the enviroGRIDS project no analysis has been done to evaluate the sensitivity of the hydrological regime to the density of weather stations in the Black Sea catchment. Generally, this step should however be undertaken prior to any study using SWAT because researchers should have in mind that one might get the right answer for the wrong reasons, this particularly with numerical models.
- Specific case studies: use available and quality-controlled local meteorological time series to drive SWAT. In order to validate SWAT, a number of outputs variables should be considered for comparison with available observations such as water discharge at a particular river outlet, etc.
- To compute the long term hydrological conditions that extend a little beyond the period of the meteorological records: that case has not been considered in the enviroGRIDS project. However, one may use the delta method with some cautions. One may also consider to “replicating” the station observation series a number of time so as to conduct a “perpetual” hydrological simulation. However, mismatches of values between the beginning and the end of the time series should then be addressed. One should also bear in mind that this perpetual simulation would not resolved other fluctuations than the “natural” variability found in the series. This method would eventually be use to “spinup” the model with regards to the hydrological variables.
- Using SWAT to compute the “long” term hydrological tendencies: one may use the “delta-method” such as that described in this report to evaluate the impact of a changing climate on the hydrology of a catchment.
- An alternate method to assess the impact of climate change in the hydrological regime within a given catchment would also make use of “raw” RCM outputs for current and for future climates without further modifications as inputs for SWAT, and regardless of what individual regime this may produce, consider only the differences in the hydrological variables. This method may be difficult to apply as the “simulated” temperature and precipitation generally have biases that impacts on the hydrology of a catchment; consequently, fine tuning of SWAT parameters may be tough to achieved.



7 References

- Boberg, F., Berg, P., Thejll, P. and Christensen, J. H., 2007. Analysis of temporal changes in precipitation intensities using PRUDENCE data. Copenhagen. Danish Meteorological Institute
- Bosshard, T., Kotlarski, S., Ewen, T. and Schar, C., 2011. Spectral representation of the annual cycle in the climate change signal. *Hydrology and Earth System Sciences*
- Christensen, J. H. and Christensen, O. B., 2007. A summary of the PRUDENCE model projections of changes in European climate by the end of this century. *Climatic Change*, vol. 81, p. 7-30
- Diaz-Nieto, J. and Wilby, R. L., 2005. A comparison of statistical downscaling and climate change factor methods: impacts on low flows in the River Thames, United Kingdom. *Climatic Change*, vol. 69, p. 245-268
- Ferro, C. A. T., Hannachi, A. and Stephenson, D. B., 2002. WP5-recommended common diagnostics for PRUDENCE: time-slice comparisons of temperature, wind speed and precipitation. The University of Reading: Department of Meteorology
- Fowler, H. J., Blenkinsop, S. and Tebaldi, C., 2007. Linking climate change modelling to impacts studies: recent advances in downscaling techniques for hydrological modelling. *International Journal of Climatology*
- Goyette, S., 2010. Existing data access and compilation on regional climate, historical records and prospects model, University of Geneva, Geneva
- Graham, L. P., Hagemann, S., Jaun, S. and Beniston, M., 2007. On interpreting hydrological change from regional climate models. *Climatic Change*, 81, 97-122
- Hanganu, J., Lehmann, A., Makarovskiy, Y., Kornilov, M., Griensven, A., Medinets, V., Mattányi, Z. and Chendes, V., 2010. Database of useful data for SWAT modeling and report on data availability and quality for hydrological modeling and water quality modeling in the Black Sea Catchments
- Hay, L. E., Wilby, R. L. and Leavesley, G. H., 2000. A comparison of delta change and downscaled GCM scenarios for three mountainous basins in the United States. *Journal of the American Water Resources Association*, vol. 36, p. 387-397
- Lenderink, G., Buishand, A. and van Deursen, W., 2007. Estimates of future discharges of the river Rhine using two scenario methodologies: direct versus delta approach. *Hydrology and Earth System Sciences*
- Mitchell, T. D., Hulme, M. and New, M., 2002. Climate data for political areas. *Area* **34**, 109-112
- Mitchell, T. D., Carter, T. R., Jones, P. D., Hulme, M. and New, M., 2003. A comprehensive set of high-resolution grids of monthly climate for Europe and the globe: the observed record (1901-2000) and 16 scenarios (2001-2100). *Journal of Climate*
- Murphy, J., 1998. An evaluation of statistical and dynamical techniques for downscaling local climate, in *Journal of Climate*, vol. 12, p. 2256-2284
- Murphy, J., 2000. Predictions of climate change over Europe using statistical and dynamical downscaling techniques. *International Journal of Climatology*, vol. 20, p. 489-501



Nakicenovic, N. , Davidson ,O., Davis, G., Grübler, A., Kram, T., la Rovere, E. L., Metz, B., Morita, T., Pepper, W., Pitcher, H., Sankovski, A., Shukla, P., Swart, R., Watson, R. and Dadi, Z., 2000. Special Report on Emissions Scenarios: A Special Report of Working Group III of the Intergovernmental Panel on Climate Change. Cambridge University Press, Cambridge, U.K., 599 pp

New, M., Hulme, M. and Jones, P., 1999. Representing Twentieth-Century Space–Time Climate Variability. Part I: Development of a 1961–90 Mean Monthly Terrestrial Climatology. American Meteorological Society, Journal of Climate, 12. Pp. 829-855.

New, M., Hulme, M. and Jones, P., 2000. Representing twentieth century space-time climate variability. Part 2: Development of 1901-96 monthly grids of terrestrial surface climate. American Meteorological Society, Journal of Climate, 13. pp. 2217-2238.

Quilbé, R., Rousseau, A., N., Moquet, J., Trinh, N. B., Dibike, Y., Gachon, P. and Chaumont, D., 2008. Assessing the effect of climate change on river flow using general circulation models and hydrological modeling application to the Chaudière River, Quebec, Canada. Canadian Water Resources Journal, vol. 33, p. 73-93

R Development Core Team (2008). R: A language and environment for statistical computing. R Foundation for Statistical Computing, Vienna, Austria.

Tapiador, F. J., Turk, F. J., Petersen, W. , Hou, A. Y., García-Ortega, E., Machado, L. A. T., Angelis, C. F., Salio, P. , Kidd, C. , Huffman, G. J. and de Castro, M., 2012. Global precipitation measurement: Methods, datasets and applications. Atmospheric Research.

University of East Anglia Climatic Research Unit (CRU). [Phil Jones, Ian Harris]. CRU Time Series (TS) high resolution gridded datasets. NCAS British Atmospheric Data Centre, 2008, 20 February 2012.